

การสร้างชิ้นงานซิลิกอนไนไตรด์พูนด้วยปฏิกิริยาकार์โบเทอร์มอลรีดักชันและไนไตรเดชันของ
อาร์เอฟซิลิกาคอมพอสิตที่ผ่านการคาร์บอนไนซ์

นางสาววิชณี จุฑาพะวงค์

วิทยานิพนธ์นี้เป็นส่วนหนึ่งของการศึกษาตามหลักสูตรปริญญาวิศวกรรมศาสตรมหาบัณฑิต

สาขาวิศวกรรมเคมี ภาควิชาวิศวกรรมเคมี

คณะวิศวกรรมศาสตร์ จุฬาลงกรณ์มหาวิทยาลัย

ปีการศึกษา 2554

ลิขสิทธิ์ของจุฬาลงกรณ์มหาวิทยาลัย

บทคัดย่อและแฟ้มข้อมูลฉบับเต็มของวิทยานิพนธ์ตั้งแต่ปีการศึกษา 2554 ที่ให้บริการในคลังปัญญาจุฬาฯ (CUIR)

เป็นแฟ้มข้อมูลของนิสิตเจ้าของวิทยานิพนธ์ที่ส่งผ่านทางบัณฑิตวิทยาลัย

The abstract and full text of theses from the academic year 2011 in Chulalongkorn University Intellectual Repository (CUIR)

are the thesis authors' files submitted through the Graduate School.

FABRICATION OF POROUS SILICON NITRIDE SPECIMEN VIA
CARBOTHERMAL REDUCTION AND NITRIDATION OF CARBONIZED
RF/SILICA COMPOSITE

Miss Wischanee Juwarahawong

A Thesis Submitted in Partial Fulfillment of the Requirements
for the Degree of Master of Engineering Program in Chemical Engineering

Department of Chemical Engineering

Faculty of Engineering

Chulalongkorn University

Academic Year 2011

Copyright of Chulalongkorn University

Thesis Title FABRICATION OF POROUS SILICON NITRIDE SPECIMEN
VIA CARBOTHERMAL REDUCTION AND NITRIDATION OF
CARBONIZED RF/SILICA COMPOSITE
By Miss Wischanee Juwarahawong
Field of study Chemical Engineering
Thesis Advisor Assistant Professor Varong Pavarajarn, Ph.D.

Accepted by the Faculty of Engineering, Chulalongkorn University in Partial
Fulfillment of the Requirements for the Master's Degree

.....Dean of the Faculty of engineering
(Associate Professor Boonsom Lerdhirunwong, Dr.Eng.)

THESIS COMMITTEE

.....Chairman
(Associate Professor Sarawut Rimdusit, Ph.D.)
.....Thesis Advisor
(Assistant Professor Varong Pavarajarn, Ph.D.)
.....Examiner
(Associate Professor Tawatchai Charinpanitkul, D.Eng.)
.....External Examiner
(Chanchana Thanachayanont, Ph.D.)

วิชณี จุวราหะวงษ์ : การสร้างชิ้นงานซิลิกอนไนไตรด์พูนด้วยปฏิกิริยาคาร์โบเทอร์มอลรีดักชัน และไนไตรเดชันของอาร์เอฟซิลิกาคอมพอสิตที่ผ่านการคาร์บอนไนซ์ (FABRICATION OF POROUS SILICON NITRIDE SPECIMEN VIA CARBOTHERMAL REDUCTION AND NITRIDATION OF CARBONIZED RF/SILICA COMPOSITE) อ. ที่ปริกษาวิทยานิพนธ์หลัก: ผศ.ดร.วรงค์ ปวราจารย์, 81 หน้า.

งานวิจัยนี้ศึกษาการสร้างชิ้นงานซิลิกอนไนไตรด์พูน โดยผสมซิลิกาเข้าไปในอาร์เอฟเจลซึ่งเตรียมด้วยเทคนิคโซล-เจล โพลีคอนเดนเซชันของเรโซซินอลกับฟอร์มัลดีไฮด์โดยใช้โซเดียมคาร์บอเนตเป็นตัวเร่งปฏิกิริยา และใช้ 3-อะมิโนโพรพิล ไตรเมทอกซิไซเลน (เอพีทีเอ็มเอส) เป็นสารตั้งต้นของซิลิกา ปฏิกิริยาระหว่างสารตั้งต้นของซิลิกากับสารละลายอาร์เอฟนั้นเกิดก่อนข้างรุนแรง และคายความร้อนเป็นอย่างมาก ทำให้สารละลายเกิดการแข็งตัวอย่างรวดเร็วจนไม่สามารถใส่สารตั้งต้นซิลิกาได้มากเท่าที่ควร ดังนั้นจึงมีการลดอุณหภูมิของอาร์เอฟเจลที่อุณหภูมิต่างๆก่อนเติมสารตั้งต้นซิลิกาและการเติมกรดอะซิติกในปริมาณที่ต่างกัน ในอาร์เอฟเจลอุณหภูมิต่ำเพื่อเป็นตัวหน่วงปฏิกิริยาเพื่อให้สามารถเติมสารตั้งต้นซิลิกาได้มากขึ้น หลังจากนั้นสารผสมจะถูกบ่มไว้อีก 72 ชั่วโมงก่อนที่จะมีการแลกเปลี่ยนตัวทำละลายในสารผสมด้วย ที-บิวทานอล ทุก 24 ชั่วโมง เป็นเวลา 3 วัน ก่อนที่จะแบ่งไปอบแห้งด้วยวิธีอบแห้งด้วยอากาศในเตาอบที่อุณหภูมิ 110 องศาเซลเซียส และวิธีอบแห้งแบบเยือกแข็งที่อุณหภูมิ -40 องศาเซลเซียส จากนั้นนำซิลิกาอาร์เอฟคอมพอสิตไปผ่านกระบวนการไพโรไลซิส ภายใต้แก๊สไนโตรเจนเพื่อกำจัดโครงสร้างอาร์เอฟให้กลายเป็นซิลิกาคาร์บอนพูนสุดท้ายผลิตภัณฑ์ที่ได้จะเข้าสู่กระบวนการไนไตรเดชันที่อุณหภูมิ 1450 องศาเซลเซียสเป็นเวลา 10 ชั่วโมง ให้กลายเป็นซิลิกอนไนไตรด์พูน แล้วเผาทำคาร์บอนส่วนเกินออกที่อุณหภูมิ 800 องศาเซลเซียสเป็นเวลา 8 ชั่วโมง จากการทดลองพบว่ากรดอะซิติกสามารถหน่วงปฏิกิริยาระหว่างอาร์เอฟเจลและสารตั้งต้นซิลิกาได้ดี เนื่องจากว่ากรดอะซิติกจะไปตัดพันธะระหว่างอาร์เอฟทำให้สามารถใส่สารตั้งต้นซิลิกาได้มากขึ้น อย่างไรก็ตาม การใส่กรดอะซิติกจำนวนมากไปจะทำให้คอมพอสิตมีความพรุนลดลง แต่ถ้าไม่มีการใส่กรดอะซิติก จะทำให้ใส่สารตั้งต้นซิลิกาได้น้อย ซึ่งทำให้โครงสร้างเปราะบางและไม่สามารถขึ้นรูปได้ ทั้งนี้การบ่มเจลที่อุณหภูมิต่างๆก่อนทำให้สามารถใส่สารตั้งต้นของซิลิกาได้มากขึ้นเนื่องจากว่าเกิดการชะลอปฏิกิริยาพอลิเมอไรเซชันที่ทำให้เกิดการเกาะกลุ่มกัน นอกจากนี้การทำสารตั้งต้นซิลิกาให้อยู่ในรูปของโซลก่อนเติมลงไปอาร์เอฟเจลก็เป็นอีกทางเลือกหนึ่งในการหน่วงปฏิกิริยา เนื่องจากซิลิกาโซลนั้นได้มีการรวมตัวให้เป็นโซลไว้ก่อนแล้วจึงทำให้เมื่อผสมลงไปอาร์เอฟที่เป็นโซลอยู่แล้ว จึงเกิดปฏิกิริยาที่ไม่รุนแรงเท่าที่เป็นสารตั้งต้นของซิลิกาเพียงอย่างเดียว

ภาควิชา.....วิศวกรรมเคมี.....ลายมือชื่อนิสิต.....
 สาขาวิชา.....วิศวกรรมเคมี.....ลายมือชื่อ อ.ที่ปริกษาวิทยานิพนธ์หลัก.....
 ปีการศึกษา...2554

5270496721: MAJOR CHEMICAL ENGINEERING

KEYWORDS: CARBOTHERMAL NITRIDATION / SILICON NITRIDE /
RESORCINOL-FORMALDEHYDE GEL

WISCHANEE JUWARAHAWONG: FABRICATION OF POROUS
SILICON NITRIDE SPECIMEN VIA CARBOTHERMAL REDUCTION
AND NITRIDATION OF CABONIZED RF/SILICA COMPOSITE.

ADVISOR: ASST. PROF. VARONG PAVARAJARN, Ph.D., 81 pp.

Introduction of silica into RF solution, which was prepared via the sol-gel polycondensation of resorcinol and formaldehyde using sodium carbonate as catalyst, was studied. 3-Aminopropyl trimethoxysilane (APTMS) was used as silica precursor. The reaction between RF solution and silica precursor is violent and extremely exothermic which results in rapid solidification of the mixture. To slow down the reaction, and to increase the amount of the silica precursor in the reaction, the reduction of temperature of RF gel and the addition of acetic acid, as inhibitor, in RF gel were used. After aging of the silica/RF gel for 72 hours, t-butanol was used in the solvent exchange process for 24 hours and repeated for 3 times. Then the sample was splitted into two parts for each drying process, i.e. convectional air drying at 110°C and freeze drying processes at -40°C. Next, the silica/RF composite was pyrolyzed under nitrogen gas to convert the RF structure into porous silica/carbon composite. Finally, the obtained product, i.e., porous silicon nitride, was obtained via carbothermal reduction and nitridation at 1450°C for 10 hours followed by the removal of excess carbon by calcination at 800°C for 8 hours. From the results, acetic acid could retard the reaction between RF gel and silica precursor because it breaks cross-linking network within RF gel, which prolongs the gelation time of the composite. However, the higher the acetic acid content is, the lower the composite porosity becomes. Without the addition of acetic acid, the composite became fragile and could not be formed into solid specimen. Aging of RF gel at low temperature also allowed more silica precursor to be added to the composite, because of the decrease in the polymerization reaction between RF and silica. Similarly, for the use of pre-formed silica sol, the silica became sol before being added into RF sol so that, the reaction was less violent.

Department: Chemical Engineering Student's Signature:.....

Field of Study: Chemical Engineering Advisor's Signature:.....

Academic Year: 2011

ACKNOWLEDGEMENTS

The authors want to dedicate all of this research to the person that relate to my successful. Assistant Professor Dr. Varong Pavarajarn, for his friendly, valuable suggestions, useful discussions throughout this research and devotion to revise this thesis; otherwise, this research work could not be completed. In addition, the author would also be grateful to Associate Professor Dr. Sarawut Rimdusit, as the chairman, Associate Professor Dr. Tawatchai Charinpanitkul, and Dr. Chanchana Thanachayanont, as the members of the thesis committee.

Most of all, the author would like to express my highest gratitude to my parents who always pay attention to me all the times for suggestions. The most success of graduation is devoted to my parents.

Finally, the author wishes to thank the member of the Center of Excellence in Particle technology, Department of Chemical Engineering, Faculty of Engineering, Chulalongkorn University for their assistance.

CONTENTS

	Page
ABSTRACT (THAI)	iv
ABSTRACT (ENGLISH)	v
ACKNOWLEDGEMENTS	vi
CONTENTS	vii
LIST OF TABLES	ix
LIST OF FIGURES	xi
CHAPTER	
I INTRODUCTION	1
II THEORY AND LITERATURE SURVEY	3
2.1 Silicon nitride	3
2.1.1 Crystal structure of silicon	4
2.1.2 Properties of silicon nitride ceramic	6
2.1.3 Carbothermal reduction and nitridation	7
2.2 Sol-gel process	9
2.3 Resorcinol Formaldehyde gel	10
2.4 Drying process	13
2.4.1 Supercritical extraction with carbon dioxide drying	13
2.4.2 Freeze drying	13
2.4.3 Drying in an inert atmosphere	14
2.5 Synthesis of porous Si ₃ N ₄ from porous silica/carbon composite	14
2.6 Interaction of RF gel with silica precursor	16
III EXPERIMENTAL	17
3.1 Materials	17
3.2 Preparation of silica/RF gel	17
3.3 Preparation of porous silica/carbon composite	18
3.4 Carbothermal reduction and nitridation	19
3.5 Characterization of the products	20
3.5.1 X-ray Diffraction Analysis (XRD)	20
3.5.2 Fourier Transform Infrared Spectroscopy (FT-IR)	21
3.5.3 Scanning Electron Microscopy (SEM)	21

	Page
3.5.4 Surface area measurement	21
3.5.5 Thermogravimetric Analysis (TGA).....	21
IV RESULTS AND DISCUSSION	22
4.1 Effect of RF aging temperature.....	23
4.1.1 Properties of pyrolyzed gel	23
4.1.2 Properties of nitrated products.....	27
4.2 Effect of acetic acid.....	32
4.2.1 Properties of pyrolyzed gel	32
4.2.2 Properties of nitrated products.....	42
4.3 Effect of drying process	48
4.3.1 Properties of pyrolyzed gel	48
4.3.2 Properties of nitrated products.....	51
4.4 The use of silica sol as silica source.....	56
4.4.1 Properties of pyrolyzed gel	57
4.4.2 Properties of nitrated products.....	61
V CONCLUSIONS AND RECOMMENDATIONS	66
5.1 Summary of the results.....	66
5.2 Conclusions	67
5.3 Recommendations for future work.....	67
REFERENCES	68
APPENDICES	73
APPENDIX A Calculation of molar ratio of silicon and carbon in RF gel composite.....	74
APPENDIX B Data of surface area and average pore diameter	76
APPENDIX C Calibration curves for gas flow meter of synthesis gas	78
APPENDIX D SEM micrographs of silicon nitride before calcinations	79
VITA.....	81

LIST OF TABLES

Table	Page
2.1	Production of silicon nitride powders 3
2.2	Typical properties of silicon nitride powders produced by various processing techniques 4
2.3	properties of silicon nitride ceramics 6
4.1	Properties silica/RF composite formed with RF gel that had been aged for 6 h at 0, 5, 10, and 25°C before being added with APTMS. 24
4.2	Surface area and pore properties of the nitrated products after calcination. The composite was prepared from RF gel aged at various temperatures without using acetic acid and subjected to freeze drying before being pyrolyzed and subsequently nitrated. The samples were divided into 2 parts, i.e. crushed powder and solid specimen before subjected to the nitridation process. 31
4.3	Maximum amount of APTMS that could be added to RF gel, based on volume of the RF gel, as a function of acetic acid content in the RF gel..... 33
4.4	Surface area and pore properties of silica/carbon composite prepared by using various amount of acetic acid. The gel was aged at 0°C before being added with APTMS..... 36
4.5	Surface area and pore properties of the nitrated products after calcination process. The composite was prepared from RF gel aged at 0°C with using various acetic acid and subjected to freeze drying before being pyrolyzed and subsequently nitrated. The samples were divided into 2 parts, i.e. crushed powder and solid specimens before subjected to the nitridation process..... 43
4.6	Surface area and pore properties of the nitrated products after calcinations process. The composite was prepared from RF gel aged at 25°C without using acetic acid and subjected to various drying before being pyrolyzed and subsequently nitrated. The samples were divided into 2 parts, i.e. crushed powder and solid specimens before subjected to the nitridation process..... 52
4.7	Composition of silica/RF composite prepared by using pre-formed silica sol as source..... 56

	Page
4.8 Surface area and pore properties of silica/RF composite prepared by using preformed silica sol.	57
4.9 Surface area and pore properties of the nitrated products after calcination process. The composite was prepared from pre-formed silica sol: 2.82 (a), 6.90 %mol (b), and RF gel aged at 0°C and subjected to various drying before being pyrolyzed and subsequently nitrated. The samples were divided into 2 parts, i.e. crushed powder and solid specimens before subjected in the nitridation process.	62
B.1 Data of surface area and average pore diameter of carbonized RF gel aged at 0°C for 6 hour with air convectional drying and freeze drying.....	76
B.2 Data of surface area and average pore diameter of carbonized RF gel aged at 25°C with air convectional drying and freeze drying.....	76
B.3 Data of surface area and average pore diameter of pure silica sol with air convectional drying.....	76
B.4 Data of surface area and average pore diameter of silica/RF composite at different temperature with fraction of acetic acid of 5.94 %mol and dried by air convectional drying.....	77
B.5 Data of surface area and average pore diameter of silica/RF composite at different temperature with fraction of acetic acid of 5.94 %mol and dried by freeze drying.	77

LIST OF FIGURES

Figure	Page
2.1	The structure of α -Si ₃ N ₄ , β -Si ₃ N ₄ and γ - Si ₃ N ₄ 5
2.2	Sol-gel process 10
2.3	Cluster growth of resorcinol-formaldehyde monomers 12
3.1	Schematic diagram of the tubular flow reactor used for the preparation of silica/carbon composite 19
3.2	Schematic diagram of the tubular flow reactor used for the carbothermal reduction and nitridation 20
4.1	SEM micrographs of pyrolyzed silica/RF composites that were dried using convectional drying process. The composites were prepared by using RF gel that had been aged at 0°C (a), 5°C (b), 10°C (c) and 25°C (d) before being added with APTMS..... 25
4.2	SEM micrographs of pyrolyzed silica/RF composites that were dried using freeze drying process. The composites were prepared by using RF gel that had been aged at 0°C (a), 5°C (b), 10°C (c) and 25°C (d) before being added with APTMS..... 26
4.3	EDX mapping for silicon in form of spherical bead particles of pyrolyzed silica/RF composites 26
4.4	XRD patterns of the nitrided products prepared from RF gel aged at 0°C (a) and 25°C (b) without using acetic acid. The composite was freeze-dried before the pyrolysis and subsequent nitridation. 27
4.5	Results of TGA analysis in oxygen atmosphere of the nitrided products prepared from RF gel aged at 0°C (a) and 25°C (b) without using acetic acid. The composite was freeze-dried before the pyrolysis and subsequent nitridation. 29
4.6	Results of TGA analysis in oxygen atmosphere of the calcined nitrided products prepared from RF gel aged at 0°C (a) and 25°C (b) without using acetic acid. The composite was freeze-dried before the pyrolysis and subsequent nitridation. 30

Page

4.7	SEM micrographs of pyrolyzed silica/RF composites that were dried using convectional drying. The composites were prepared by using RF gel added with acetic acid in the amount of 0 (a), 24.01 (b), 30.67 (c) and 36.26 %mol (d). The gel was formed at room temperature.	33
4.8	SEM micrographs of pyrolyzed silica/RF composites that were dried using convectional drying process. The composites were prepared by using RF gel added with acetic acid in the amount of 5.94%mol. The gel was formed at 0°C (a), 5°C (b), 10°C (c) and 25°C (d).	34
4.9	SEM micrographs of pyrolyzed silica/RF composites that were dried using freeze drying process. The composites were prepared by using RF gel added with acetic acid in the amount of 5.94 %mol. The gel was formed at 0°C (a), 5°C (b), 10°C (c) and 25°C (d)	35
4.10	SEM micrographs of pyrolyzed silica/RF composites that were dried using convectional drying. The composites were prepared by using RF gel added with acetic acid in the amount of 1.25 (a), 2.47 (b), 3.65 (c) and 4.81 %mol (d) ...	37
4.11	SEM micrographs of pyrolyzed silica/RF composites that were dried using freeze drying. The composites were prepared by using RF gel added with acetic acid in the amount of 1.25 (a), 2.47 (b), 3.65 (c) and 4.81 %mol (d)	38
4.12	FTIR spectra of silica/RF composites prepared by using RF gel with acetic acid content of 0 (a), 24.01 (b), 30.67 (c) and 36.26 %mol (d).....	40
4.13	Results of TGA analysis of the sample prepared with the acetic acid content of 2.47 %mol, after being freeze-dried (a) and after being pyrolyzed (b)	41
4.14	XRD patterns of the nitrated products prepared from RF gel using acetic acid content of 2.47 (a) and 5.94 %mol (b). The composite was freeze-dried before the pyrolysis and subsequently nitridation.....	42
4.15	Results of TGA analysis in oxygen atmosphere of the nitrated products fabricated from the gel prepared at 0°C, using acetic acid content of: 2.47 (a) and 5.94 %mol (b).....	44
4.16	Results of TGA analysis in oxygen atmosphere of the final calcined products fabricated from the gel prepared at 0°C, using acetic acid content of: 2.47 (a) and 5.94 %mol (b).....	45

	Page
4.17 SEM micrographs of the nitrated product in the form of solid piece, prepared from RF gel with acetic acid content of 2.47 %mol. The micrographs were taken at the surface (a) and in the center (b) of the specimen.	46
4.18 SEM micrographs of the nitrated product in the form of solid piece, prepared from RF gel with acetic acid content of 2.47 %mol. The micrographs were taken in the center of the specimen.	47
4.19 Relationship between the content of acetic acid and surface area of silica/carbon composite prepared by using different drying process.	49
4.20 Relationship between the content of acetic acid and pore volume of silica/carbon composite prepared by using different drying process.	49
4.21 Pore size distribution of silica/carbon composite prepared by using different acetic acid content. The composites were dried by convectional drying process.	50
4.22 Pore size distribution of silica/carbon composite prepared by using different acetic acid content. The composites were dried by freeze drying process.	50
4.23 XRD patterns of the nitrated products prepared from RF gel without using acetic acid. The composites were prepared by convectional (a) and freeze-drying (b) process.	51
4.24 Results of TGA analysis in oxygen atmosphere of the nitrated products prepared from RF gel aged at 25°C without using acetic acid. The samples were nitride in different formed: (a) powder prepared by convectional drying, (b) solid piece prepared by convectional drying, (c) powder prepared by freeze drying and (d) solid piece prepared by freeze drying.	54
4.25 Results of TGA analysis in oxygen atmosphere of the calcined nitrated products prepared from RF gel aged at 25°C without using acetic acid. The samples were nitride in different formed: (a) powder prepared by convectional drying, (b) solid piece prepared by convectional drying, (c) powder prepared by freeze drying and (d) solid piece prepared by freeze drying.	55
4.26 SEM micrographs of pyrolyzed pre-formed silica sol/RF composites that were dried using convectional drying. The composites were prepared by using RF with different silica content of 2.82 (a), 6.21 (b), 6.56 (c) and 6.90 %mol (d).	58

	Page
4.27 SEM micrographs of pyrolyzed pre-formed silica sol/RF composites that were dried using freeze drying. The composites were prepared by using RF with different silica content of 2.82 (a), 6.21 (b), 6.56 (c) and 6.90 %mol (d).....	59
4.28 FTIR spectra of silica/RF composites prepared by using preformed silica sol with various compositions: (a) RF-EtOH without acetic acid, (b) RF-EtOH-SiO ₂ without acetic acid, (c) RF-EtOH-SiO ₂ with acetic acid, (d) RF-SiO ₂ with acetic acid.	60
4.29 XRD patterns of the nitrated products prepared from pre-formed silica sol; 2.82 (a) and 6.90 %mol (b), and RF gel with using acetic acid of 5.94 %mol. The composite was freeze-dried before the pyrolysis and subsequently nitridation.	61
4.30 SEM micrographs of the nitrated product in the form of solid piece, prepared from pre-formed silica sol with the silica content of 2.82 %vol. and RF gel without using acetic acid. The micrographs were taken at the surface (a) and in the center (b) of the specimen.	64
4.31 SEM micrographs of the nitrated product in the form of solid piece, prepared from pre-formed silica sol with the silica content of 6.90 %vol. and RF gel with acetic acid content of 5.94 %vol. The micrographs were taken in the center of the specimen.	65
C.1 The calibration curve for argon.....	78
C.2 The calibration curve for nitrogen.....	78
D.1 SEM micrograph of silicon nitride powder by RF/silica composite with fraction of acetic acid of 2.47 %mol dried by freeze drying.....	79
D.2 Photograph of silicon nitride powder synthesized by RF/silica composite with fraction of acetic acid of 2.47 %mol dried by freeze drying.....	80

CHAPTER I

INTRODUCTION

Silicon nitride (Si_3N_4) is one of the most promising ceramic materials because of its high temperature strength, thermal shock resistance, chemical stability and excellent creep resistance that are of interest for several engineering applications, such as gas filter, gas turbine, separation membranes, wear-resistance materials and catalyst supports [1-3]. Silicon nitride powder does not exist in nature. It can be fabricated following these techniques: (1) direct nitridation of silicon, (2) carbothermal reduction and nitridation of silica, (3) vapor phase synthesis, (4) thermal decomposition of silicon diimide, etc [4]. The first and the second techniques are the most popular technique used in many industries.

Porous ceramics have also been attracting great interest for various applications relating to separation in severe environments, in which materials such as metals or organic materials cannot be used. Porous ceramic thin films with fine pores are candidate materials for the separation of specific gas, liquid and solid phases under high temperature or high corrosive environments.

Recent research interest has been shifted toward the formation of porous silicon nitride. Properties of the porous silicon nitride ceramics are influenced by their relative density and grain and pore morphology (grain size, aspect ratio, pore size and amount) [5]. The porous silicon nitride ceramics has been successfully prepared by partial sintering, restrained sintering, tape casting, partial hot-pressing, partial forge sintering, and addition of fugitive inclusions. Most of these processes required α -silicon nitride powder as the starting powder because densification and sintering of α -silicon nitride powder is much easier than sintering of β -powder [6, 7].

RF gel was first produced from resorcinol and formaldehyde by Pekala [8] and it can be converted into highly porous carbon gel by pyrolyzation. RF gel is favorable for the production of the carbon gel because of high porosity, large surface area, and controllable pore size distribution. So, it is used in many applications. In this work, it is intended to use as a source of carbon for the synthesis of silicon nitride via carbothermal reduction and nitridation technique.

In this research, porous silicon nitride is synthesized by the carbothermal reduction and nitridation of the silica/carbon composite which is formed by a pyrolyzed composite of silica/RF gel. Nevertheless, according to past researches, the content of silica that can be added to RF gel is limited by a spontaneous reaction between silicon precursor and RF gel, which consequently results in rapid solidification of the gel. Therefore, this work focuses on the effect of an inhibitor, i.e., acetic acid, temperature, activity of silica precursor, on the amount of silica that can be added to form the silica/RF composite.

This thesis is divided into five chapters. The first three chapters describe general information about the study, while the following two chapters emphasize on the results and discussion from the present study. Chapter I is the introduction of this work. Chapter II describes basic theory about silicon nitride such the general properties of titania, carbothermal reduction and nitridation, sol-gel process, resorcinol–formaldehyde (RF) gel, drying processes, synthesis of porous silicon nitride from porous silica/carbon composite and interaction of RF gel with silica precursor. Chapter III shows materials and experimental systems. Chapter IV presents the experimental results and discussion. In the last chapter, the overall conclusion from the results and recommendation for future work are presented.

CHAPTER II

THEORY AND LITERATURE SURVEY

2.1 Silicon nitride

Silicon nitride (Si_3N_4) is the one of the most promising engineering ceramic materials. It does not exist in nature and has to be fabricated. These characteristics are very important for the excellent silicon nitride [2]. The following techniques are usually applied to synthesize silicon nitride powder: (1) direct nitridation of silicon, (2) carbothermal reduction and nitridation of silica, (3) thermal decomposition of silicon diimide, and (4) gas-phase reaction of silane, (5) plasmachemical synthesis, (6) pyrolyses of silicon organic compounds, and (7) laser induced reactions. All of these routes are based on four different chemical processes, as shown in Table 2.1.

Table 2.1 Production of Si_3N_4 powders.

Method	Chemical process
Direct nitridation	$3\text{Si} + 2\text{N}_2 \rightarrow \text{Si}_3\text{N}_4$
Carbothermal nitridation	$3\text{SiO}_2 + 6\text{C} + 2\text{N}_2 \rightarrow \text{Si}_3\text{N}_4 + 6\text{CO}$
Diimide synthesis	$\text{SiCl}_4 + 6\text{NH}_3 \rightarrow \text{Si}(\text{NH})_2 + 4\text{NH}_4\text{Cl}$ $3\text{Si}(\text{NH})_2 \rightarrow \text{Si}_3\text{N}_4 + 3\text{NH}_3$
Vapor phase synthesis	$3\text{SiCl}_4 + 4\text{NH}_3 \rightarrow \text{Si}_3\text{N}_4 + 12\text{HCl}$

For the industrial production of silicon nitride, silica, silicon and silicon tetrachloride (SiCl_4) are three commonly used starting materials for these processes. However, properties of the powders produced may be changed by conditions of these various techniques as shown in Table 2.2 [4].

Table 2.2 Typical properties of silicon nitride powders produced by various processing techniques.

Properties	Direct nitridation of silicon	Vapor phase synthesis	Carbothermal nitridation	Diimide synthesis
Specific surface area (m ² /g)	8-25	3.7	4.8	10
Oxygen content (wt %)	1.0-2.0	1	1.6	1.4
Carbon content (wt %)	0.1-0.4	-	0.9-1.1	0.1
Metallic impurities (wt %)	0.07-0.15	0.03	0.06	0.005
Crystallinity (%)	100	60	100	100
$\alpha/(\alpha+\beta)$ (%)	95	95	95	85

2.1.1 Crystal structure of silicon nitride

Initially, the crystal structure of silicon nitride was designated as α - and β - Si_3N_4 since these phases can be produced under normal nitrogen pressure. Their crystal structures are shown in Figure 2.1. However, by the recent discovery, γ - Si_3N_4 can also be formed only at extremely high nitrogen pressure [9]. Nevertheless, α - and β -phases are more favorable than γ -phase because γ -phase has no practical use yet. The α -phase is the generally preferred as raw material for manufacturing compact

bodies because of the favorable micro structural characteristics obtained during the phase transformation into β -phase at high temperature. β - Si_3N_4 is thermodynamically more stable phase at all temperatures and therefore the transformation from β to α -phase is not possible. In the mid-1950s, detailed X-ray diffraction (XRD) has proved that the crystal structure of both α and β polymorphs are hexagonal. The basic unit form of Si_3N_4 is the Si-N tetrahedron which silicon atom is at the centre of a tetrahedron with four nitrogen atom at each corner. However, their respective structural dimensions are different [10, 11].

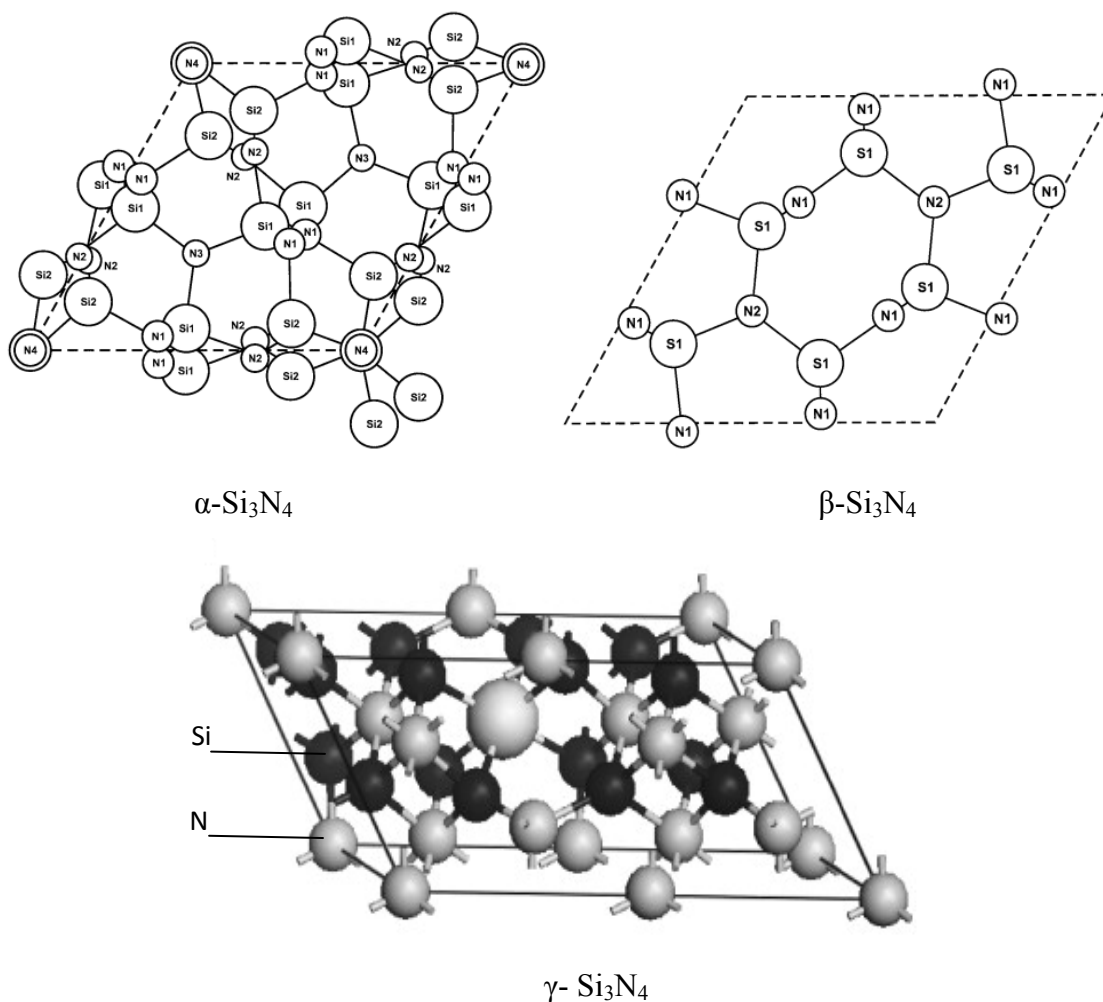


Figure 2.1: The structure of α - Si_3N_4 , β - Si_3N_4 and γ - Si_3N_4 [12, 13].

2.1.2 Properties of silicon nitride ceramic

Properties of silicon nitride ceramics depend on type of silicon nitride, i.e., dense silicon nitride produced by hot-pressing [14, 15], sintering or hot-isostatic pressing [16, 17], and porous silicon nitride produced by reaction-bonding of silicon powder compacts [18]. The properties of two types of silicon nitride specimens are shown in Table 2.3 [17].

Table 2.3 Properties of silicon nitride ceramics.

Theoretical density (g cm^{-3}): α -phase β -phase	3.168-3.188 3.19-3.202
Density (g cm^{-3}): dense Si_3N_4 reaction-bonded Si_3N_4	90-100% th.d.* 70-88% th.d.
Coefficient of thermal expansion (20-1500°C) (10^{-6}C^{-1})	2.9-3.6
Thermal conductivity (RT) ($\text{W m}^{-1}\text{K}^{-1}$): dense Si_3N_4 reaction-bonded Si_3N_4	15-50 4-30
Thermal diffusivity (RT) ($\text{cm}^2 \text{sec}^{-1}$): dense Si_3N_4 reaction-bonded Si_3N_4	0.08-0.29 0.02-0.22
Specific heat ($\text{J kg}^{-1} \text{ }^\circ\text{C}^{-1}$)	700
Electrical resistivity (RT) ($\Omega \text{ cm}$)	$\sim 10^{13}$
Microhardness (Vickers, MN m^{-2})	1600-2200

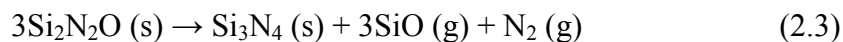
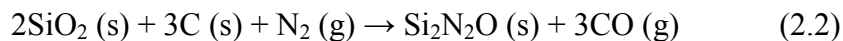
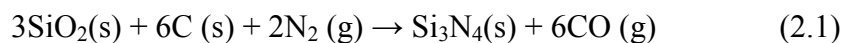
Table 2.3 (continued)

Young's modulus, (RT) (GN m^{-2}):	
dense Si_3N_4	300-330
reaction-bonded Si_3N_4	120-220
Flexural strength (RT) (MN/m^2):	
dense Si_3N_4	400-95
reaction-bonded Si_3N_4	150-350
Fracture toughness ($\text{MN m}^{-3/2}$):	
dense Si_3N_4	3.4-8.2
reaction-bonded Si_3N_4	1.5-2.8
Thermal stress resistance parameter $R = \sigma_F(1-\nu)/\alpha E$ ($^{\circ}\text{C}$) and $R' = R\lambda$ (10^3 W m^{-1}):	
dense Si_3N_4	$R = 300-780$ $R' = 7-32$
reaction-bonded Si_3N_4	$R = 220-580$ $R' = 0.5-10$

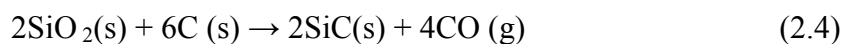
th.d.* = Theoretical density is dependent on the type and composition of consolidation aids (th.d. = Theoretical density of pure $\text{Si}_3\text{N}_4 = 3.2 \text{ g cm}^{-3}$)

2.1.3 Carbothermal reduction and nitridation of silica

The carbothermal reduction and nitridation is one of the easiest methods to synthesize silicon nitride. The process involves simultaneous reduction of silica by carbon and reaction with nitrogen at temperature in the range from 1400°C up to 1500°C . The overall reaction for the carbothermal synthesis of silicon nitride can be written as [19]:



At high temperature, the carbothermal nitridation reaction can produce either α - Si_3N_4 or β - Si_3N_4 . Nevertheless, as the carbon is an active reducer of oxide, SiO_2 can react with the carbon directly to form SiC [20]. The SiC formation can be prevented by controlling high partial pressure of nitrogen gas to promote the Si_3N_4 formation [20].



α - Si_3N_4 can be produced directly from very fine grain silica and carbon at temperature in the range of 1200-1450°C depending on the reactivity of raw materials and C/ SiO_2 ratio [19]. In some processes, sintering additives such as Y_2O_3 , MgO, and Al_2O_3 are used to reduce the time of reaction and changing the morphology of silicon nitride product [21, 22]. At temperature above 1600°C, the phase transformation from α - Si_3N_4 to β - Si_3N_4 will occur [7, 23].

Carbothermal reduction and nitridation process produces powder with >95% α - Si_3N_4 phase. The reaction is moderately exothermic with activation energy of 457±55 kJ/mol. The reaction requires 4-5 h to complete [19]. This synthesis method was used because the porous silicon nitride can be obtained by using the porous carbon. Resorcinol formaldehyde gel was used in this research, as a template of carbon source.

2.2 *Sol-gel process*

Sol-gel process is a wet chemical technique for the synthesis of materials starting from chemical solution to produce an integrated network which undergoes hydrolysis and polycondensation reactions to form colloid or “sol”, according to Equation 2.5 to 2.7 where M and R are metal atom and alkyl groups, respectively.



In general, the sol-gel process involves the transition of a solution system from liquid “sol” into solid “gel” phase. For the sol-gel process, as shown in Figure 2.2, it is possible to fabricate materials in a wide variety of forms, e.g. ultra-fine or spherical shaped powders, thin film coatings, fibers, porous or dense materials, and extremely porous aerogel.

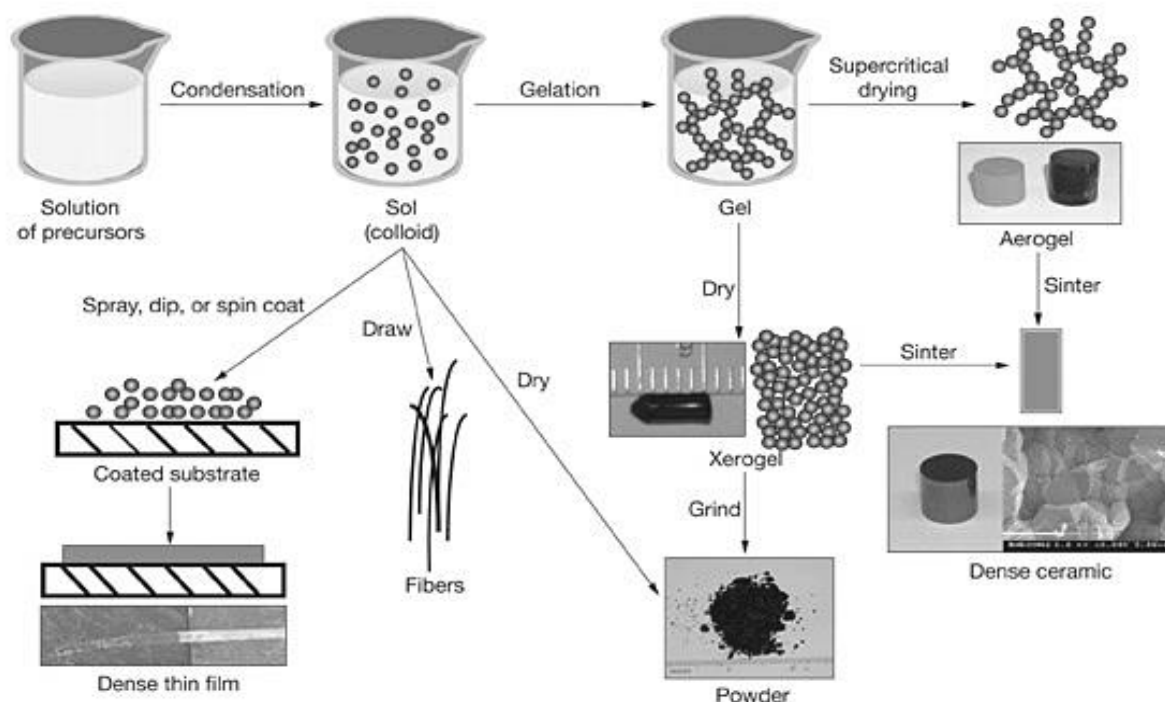


Figure 2.2: Sol-gel process.

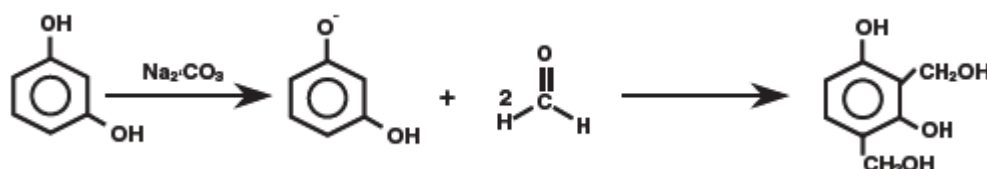
2.3 *Resorcinol Formaldehyde gel*

RF gel is an attractive porous material with moderately high surface area and large mesopore volume. Carbon xerogel can be prepared by pyrolyzing RF gel in an inert gas atmosphere and can be used for many applications such as adsorbents, electrodes for electric double layer capacitors, catalyst supports, and materials for hydrophobic chromatographic separation [24].

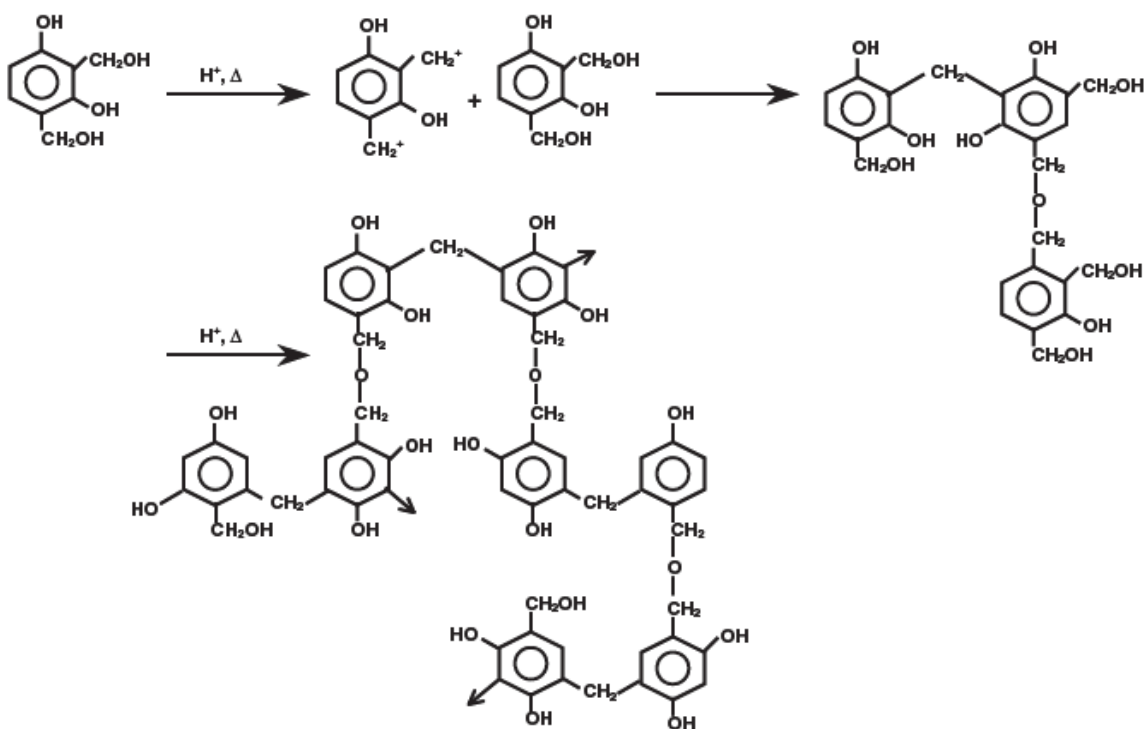
RF gel was firstly produced by Pelaka via the sol-gel polycondensation of resorcinol (R) and formaldehyde (F) using sodium carbonate (C) as basic catalyst, and distilled water as diluents [8]. The major reactions between resorcinol and formaldehyde include (1) the addition reaction to form hydroxymethyl derivatives ($-\text{CH}_2\text{OH}$) of resorcinol, and (2) the condensation reaction of the hydroxymethyl

derivatives to form methylene (-CH₂-) and methylene ether (-CH₂OCH₂-) bridged compounds [25, 26].

(1) Addition reaction



(2) Condensation reaction



The porous structure of RF aerogels depends on the amount of resorcinol, basic catalyst, and water used in the sol-gel polycondensation. The catalyst is one of the most important factors affecting properties of the product. The catalyst initially promotes the generation of resorcinol anions. These anions are subsequently transformed into substituted resorcinols which form RF clusters through polycondensation. Then RF clusters react with each other and grow into colloidal particles which finally form a RF hydrogel (Figure 2.3) [26, 27].

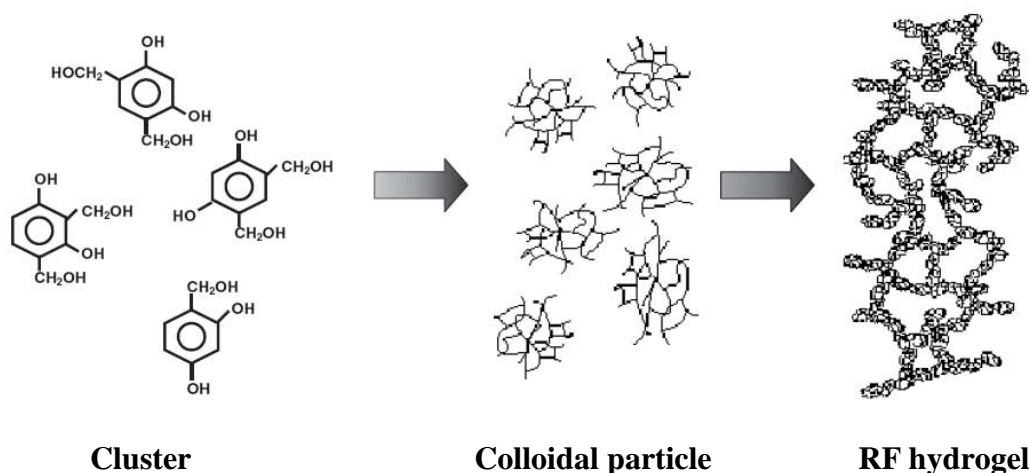


Figure 2.3: Cluster growth of resorcinol-formaldehyde monomers.

Many researchers have used RF gel as a source of porous carbon because its porosity, pore size distribution, shrinkage, and mechanical properties can be controlled by varying many synthesis factors of RF gel such as R/C, R/F, and R/W molar ratios. Leonard et al. had controlled R/C ratio in the range of 300-1500 and found that R/C molar ratio greatly influences the shrinkage and mechanical properties. With smaller R/C ratio, the higher shrinkage, stiffening, and the viscoelastic character of xerogels are obtained. Higher R/C ratio tends to give mesopores within the sample [28]. Yoshimune et al. and Siyasukh et al. discovered that large C/W ratio results in small pore size [29, 30]. Tamon et al. reported the effect of R/C, R/W and R/F ratios on porous structure that (1) low R/C or high R/W values yields monodisperse porous structures; (2) increasing of R/C ratio or decreasing of R/W ratio results in dispersed pore size distribution of the aerogel; (3) the surface area of the sample can be controlled by adjusting R/C ratio, while its mesopore volume changes greatly with R/C or R/W ratios [25]. Effects of other factors, i.e. stirring speed and viscosity of RF gel were investigated by Horikawa et al. The results showed that viscosity of RF gel can control particles size and particles spherical shape. With increasing viscosity, fine spheres with increased size will be obtained. Moreover; small particles will be acquired if high stirring speed is used [31].

2.4 *Drying processes*

Drying process is one of the factors effecting porosity of RF gel. Pore structure and surface area of the final carbon derived from RF gel depend not only on the synthesis conditions of RF gel but also on the drying and carbonizing techniques. There are many kinds of drying method to convert hydrogel to a solid RF gel such as evaporation drying, the convective hot gas drying, the microwave drying and the vacuum drying [32]. Conventionally, there are three well-known drying methods that are favorable [24].

2.4.1 Supercritical extraction with carbon dioxide

This method is the most useful for obtaining mesoporous RF gels, but its cost is extremely high. Acetone is firstly used in the solvent exchange process. Then, it is replaced by liquid carbon dioxide in the reactor. This technique gives RF aerogel with an intermediate surface area [33]. Liang et al. prepared RF aerogels using the supercritical acetone drying and compared with RF aerogels obtained from supercritical carbon dioxide drying. It was found that the suitable temperature and pressure of the supercritical acetone drying could avoid the collapse of the organic gel structure during the drying process. The chemical composition and the morphology of the organic aerogels obtained from the supercritical acetone drying were similar to the aerogels from supercritical carbon dioxide drying, but the pore size was larger than that prepared from supercritical carbon dioxide drying [34].

2.4.2 Freeze drying

Freeze drying is an effective way to preparing high surface area specimen with controlled pore structure. This process is less expensive compared with supercritical extraction with carbon dioxide. Moreover, the surface area and the pore volume are largest for RF cryogels. Shrinkage of the gels is also the minimized. t-Butanol is used for the solvent exchange process instead of acetone because the freezing point of

acetone is lower than the temperature of the freeze drying process. Pre-freezing period before drying is necessary. The gel is pre-cooled for 1 day at -20°C . The frozen gel is transferred into freeze drying apparatus, where the temperature is reduced to -45°C . Tamon et al. prepared mesoporous carbon cryogel freeze drying. The obtained RF cryogels had mesopore volumes larger than $0.58\text{ cm}^3/\text{g}$ and carbon cryogels were found to be mesoporous with high surface area $> 800\text{ m}^2/\text{g}$ and mesopore volume $> 0.55\text{ cm}^3/\text{g}$. Besides, it was also found that, when pyrolyzed, micropores were formed inside the cryogels more easily than inside the aerogels. Although surface areas and mesopore volumes of the cryogels were smaller than the aerogels, the cryogels were useful precursors of mesoporous carbons [35].

2.4.3 Convective air drying

This is the simplest way to convert the RF hydrogel into a solid gel. However the surface area, pore volume and mean pore diameter of the xerogel are smaller than those of aerogel and cryogel. Some researchers such as Czakkel et al. and Job et al. used this drying technique with the solvent exchange process by acetone. The obtained xerogels had the most compact structure with the lowest specific surface area when compared with aerogels and cryogels in the same experiment [36, 37].

2.5 *Synthesis of porous Si_3N_4 from porous silica/carbon composite*

Porous silicon nitride can be fabricated from silica incorporated into porous carbon via the carbothermal reduction and nitridation process. The production of porous silica/carbon composite has been reported by Aguado et al. and Xu et al., using RF/TEOS mixture. Aguado found that there were many parameters which affected porosity, such as, pH value water content and silica content, At pH ~ 3 the product was macroporous solid while at basic pH (~ 7) the pores were essentially microporous. The most significant change produced in the silica/RF xerogels when the pH was increased the decrease in the mesopore volume. For the water content, the mesopore volume increased significantly only for $\text{R/W} > 2$. For the silica content, the

increased amount of silica in the composites, in general, decreased the macroporosity and increased the mesoporosity. Xu et al. was also studied the effect of increasing silica content. The gelation time was greatly reduced with increasing TEOS content, that indicating the interaction of the organic/inorganic precursors was favorable for the formation of cross-linking networks. However, excessive increase of TEOS content led to increased shrinkage and the sharp increase of apparent density of RF/silica composite gels. Besides, with increasing amount of TEOS, the cross-section morphology was changed from roughness to smoothness and decreasing of macropore volume [38, 39]. Beside RF gel, other materials such as phenol [40], furfural [40], and polyfurfuryl alcohol (PFA) [41] have also been used as source the porous carbon. Zarbin et al. applied PFA and porous vycor glass (PVG) to form PFA/porous glass nanocomposite [42]. For the synthesis of porous silicon nitride, Luyjew et al. synthesized mesoporous silicon nitride from carbonized silica/RF gel composite via the carbothermal reduction and nitridation process. APTMS was used as a silica precursor because it has suitable structure from crosslinked Si-O-Si network, which can produce silicon nitride during the carbothermal reduction and nitridation, more than TEOS. Silica to carbon ratio has influence on surface area of silicon nitride product. The lower Si/C ratio produces low surface area product, while higher Si/C leads to the stronger pore structure and high surface area [43]. Moreover, porous carbon derived from phenolic resin has also been used to generate porous silicon carbide/silicon nitride composite ceramics with high flexural strength and high porosity up to 63% [44].

2.6 *Interaction of RF gel with silica precursor*

Due to the good properties of RF gel, many researchers have studied the method to adjust RF gel with vary substance. Thovicha [45] incorporated titania into structure of RF gel via sol-gel process. However, the reaction between titania precursor and RF solution is quite violent and extremely exothermic, resulting in rapid solidification of the gel. So, the conversion of the precursor into preformed titania sol to decrease its reactivity was proposed. There were two processes in the reaction between titania sol and RF solution. One was reaction between RF cluster and titania sol. The other one was interaction of titania sol. The titania sol reacted with RF gel at methylene ether bridge and formed into cross-linking network. Besides, Poumuang [46] studied incorporation of silica into RF gel. The reaction between silica precursor and RF solution is also strongly exothermic as observed in the case of titania. Thus, to increase amount of silica that can be added into RF gel, acetic acid was added to destabilize methylene and methylene ether bridges network. The result showed that silica precursor incorporated into RF clusters at positions of hydroxyl group.

CHAPTER III

EXPERIMENTAL

This chapter describes the experimental procedure in this research. This chapter is separated into five sections; raw materials, preparation of silica/RF gel, preparation of silica/carbon composite, carbothermal nitridation and characterization of the products.

3.1 *Materials*

Resorcinol 99.8% (R) and formaldehyde solution 37% (F) were used to prepare RF gel. Sodium carbonate anhydrous 99.8% (Na_2CO_3) was used as a catalyst for RF gel preparation. 3-Amino propyl trimethoxysilane 97% (APTMS) was used as a precursor for silica. Acetic acid 99.8% (CH_3COOH) was used as an inhibitor.

Resorcinol, formaldehyde solution, sodium carbonate anhydrous and acetic acid were purchased from Asia Pacific Specialty Chemicals Limited. APTMS was purchased from Sigma-Aldrich Chemical Company. All chemicals were used as received without further purification.

3.2 *Preparation of silica/RF gel*

Silica/RF gel was prepared from resorcinol (R), formaldehyde (F), sodium carbonate (C) and distilled water (W), using R/F molar ratio of 0.5, R/W molar ratio of 0.15 and C/W ratio of 10 mol/dm³. At first, 2.7 g resorcinol was dissolved in 2.67 ml distilled water and stirred until it dissolved completely. Next, 0.3 ml of 10 M sodium carbonate in distilled water solution was added into the solution and stirred at room temperature for 15 minutes. After that, 3.75 ml of formaldehyde solution was

added and stirred for 15 minutes. Then, acetic acid, which was varied in amount from 0.2, 0.4, 0.6, 0.8, and 1 ml, was added before adding APTMS into the solution under continuous stirring. The mixture was aged at the room temperature for three days. After aging, the obtained gel was divided into three parts. The first part was immediately dried in an oven at 110°C for 24 h. The second part was freeze-dried at -40°C. The last portion was underwent through the solvent exchange process by immersing the sample in 50 ml of t-butanol for 3 days, renewed with fresh t-butanol everyday. Then the sample was split into two parts for each drying process, i.e. convectional drying and freeze drying processes.

In some experiments, effects of temperature and reactivity of the precursor were investigated. For the effect of temperature, the gel after being added with formaldehyde was aged at 0, 5, 10, and 25°C for 6 h. The aged gel was then added with APTMS under continuous stirring without the addition of acetic acid. For the effect of reactivity of the precursor, APTMS was converted into silica sol to retard its reactivity before being added into the RF solution at controlled temperature of 0°C. The mixtures were aged and dried in the same manner as previously described.

3.3 *Preparation of porous silica/carbon composite*

Porous silica/carbon composite was obtained by pyrolysis of the dried silica/RF gel in the step-wised fashion from 250°C to 750°C under continuous flow of nitrogen (15 ml/min) in a horizontal furnace (Figure 3.1). The dried silica/RF gel was firstly heated to 250°C at a constant heating rate of 10°C/min and held for 2 h. Then it was heated up to 750°C at the same heating rate and held for 4 h. The product of this step is silica/carbon composite.

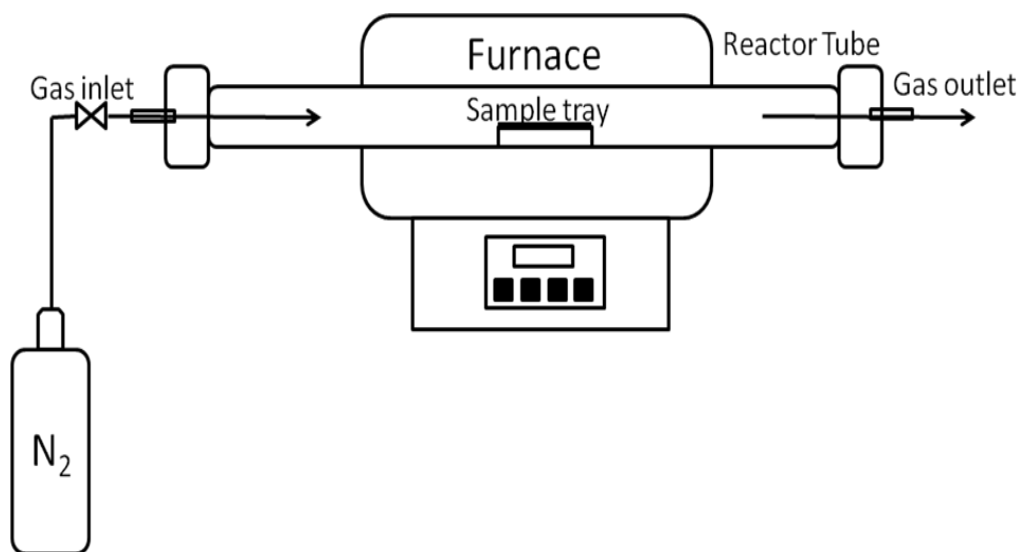


Figure 3.1: Schematic diagram of the tubular flow reactor used for the preparation of silica/carbon composite.

3.4 Carbothermal reduction and nitridation

This process was started by putting the silica/carbon composite into an alumina tray (25 mm x 15 mm x 5 mm deep) and placing it in a horizontal tubular flow reactor. The schematic diagram of the reactor system is shown in Figure 3.2. The composite was then heated to 1450°C at the heating rate of 10°C/min under continuous flow of argon at 50 l/min. After the temperature had reached 1450°C, the gas stream was switched from argon to a mixture of 90% nitrogen and 10% hydrogen with total flow rate of 50 l/min. The reaction was held at constant temperature for 10 h. The obtained product was then calcined in a box furnace at 700°C for 10 h to remove excess carbon.

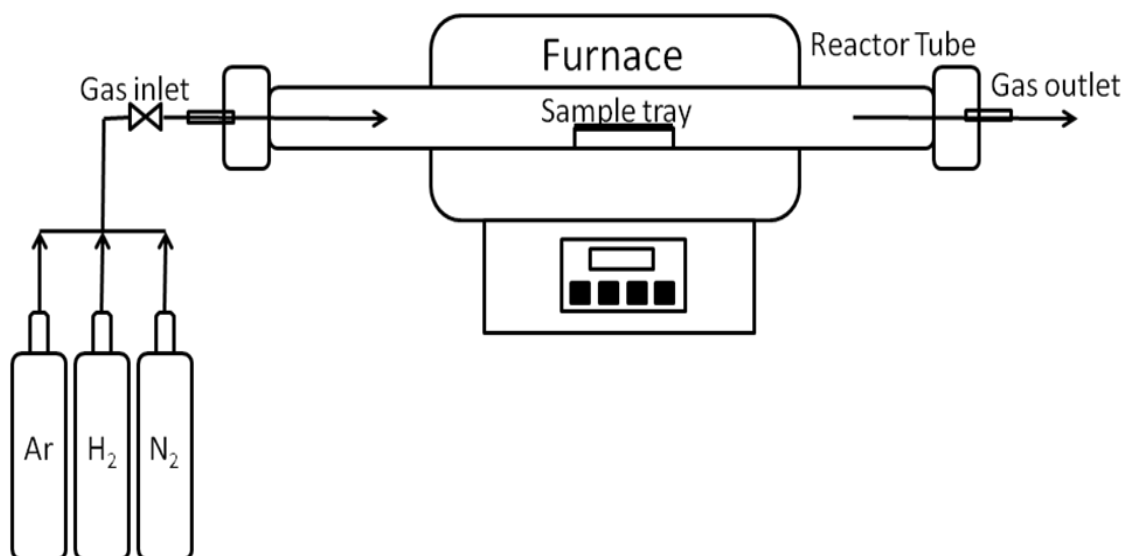


Figure 3.2: Schematic diagram of the tubular flow reactor used for the carbothermal reduction and nitridation.

3.5 Characterizations of the products

The obtained products were characterized by using various techniques, as following:

3.5.1 X-ray Diffraction analysis (XRD)

Crystalline phases of the product were determined from X-ray diffraction analysis, using a SIEMENS D5000 diffractometer with $\text{CuK}\alpha$ radiation. Each sample was scanned in the range of $2\theta = 10\text{-}50^\circ$ with a step size of $2\theta = 0.02^\circ$.

3.5.2 Fourier-Transform Infrared Spectroscopy (FT-IR)

The functional groups in the samples were determined by using a Perkin Elmer (Spectrum One) infrared spectrometer. The sample was mixed with KBr with the sample to KBr ratio of 1:100 and formed into a thin pellet, before measurement. The spectra were recorded at wavenumber between 400 and 4000 cm^{-1} with resolution of 4 cm^{-1} . The number of scan for the measurement was 64.

3.5.3 Scanning Electron Microscopy (SEM)

Morphology of the products was examined by using a scanning electron microscope (JSM-6400, JEOL Co., Ltd.) at the Scientific and Technological Research Equipment Center (STREC), Chulalongkorn University.

3.5.4 Surface area measurement

BET surface area of products was measured by Belsorp mini II BEL, Japan at Center of Excellence in Particle and Technology Engineering laboratory, Chulalongkorn University. For this measurement nitrogen gas was used as the adsorbate. The samples were preheated at 150°C for 3-4 h, before measurement.

3.5.5 Thermogravimetric Analysis (TGA)

The residual carbon content and thermal behavior of the samples were determined by using thermogravimetric analysis on a Mettler-Toledo TGA/DSC1 STAR^e System. The analysis was performed from temperature of 25 to 1,000°C under a heating rate of 10°C/min in 100 ml/min of oxygen.

CHAPTER IV

RESULTS AND DISCUSSION

In this chapter, properties of pyrolyzed silica/RF composite and those of nitrated product are investigated. Effects of various factors, including solvent exchange, acetic acid, temperature, drying process, as well as source of silica, are presented. It should be noted that the pyrolyzed products with maximum silica content and maximum surface area were chosen in the study of effects mentioned above because it is a main objective of this thesis to form the porous monolith product which needs the highest silica content and surface area.

According to the spontaneous reaction between APTMS and RF gel, as witnessed from rapid solidification and violently exothermic behavior, the amount of APTMS that could be added to the RF gel is limited. After adding silica precursor into RF gel without adjusting pH value (native pH of RF gel is c.a. 6.4-7.4 [38]) at the room temperature, the gel was immediately solidified. So, high content of silica could not be added to the RF gel under normal synthesis conditions. The addition of acetic acid, decreasing of temperature and using pre-formed silica sol as the source were means to increase the amount of silica in the composite. On the other hand, type of drying process was studied to increase surface area of the composite. According to preliminary experiments, it was found that solvent exchange process also increased the surface area of the composite. So the solvent exchange process was used in all experiments.

4.1 *Effect of RF aging temperature*

In this section, RF gel was aged at different temperature (i.e., 0°C, 5°C, 10°C, and 25°C) before being added with APTMS, without using acetic acid as inhibitor. The aging time of 6 h was used because, according to the preliminary experiment, the long period of aging time at 0°C (i.e. 24 h) allowed less silica content to be added than the short period of aging time (i.e. 6 h).

4.1.1 Properties of pyrolyzed gel

Table 4.1 shows properties of the pyrolyzed gel synthesized from APTMS and RF gel aged at different temperature. The lowering of the gel temperature could retard the violent reaction between APTMS and RF gel so that rapid solidification of the gel could be avoided. However, the rise in temperature of the gel after being added with APTMS was still observed. At higher temperature, the gelation process can occur more rapidly because the polymerization reaction is enhanced. According to Arrhenius equation, rate constant increases with increasing temperature resulting in increasing in the reaction between RF-gel and APTMS [26]. SEM micrographs of the pyrolyzed composites fabricated using conventional and freeze-drying are shown in Figure 4.1 and Figure 4.2, respectively. Higher temperature favors hydrolysis reaction, which is endothermic, and results in shorter gelation time and therefore less compact structures with wider pores [47]. Figure 4.1(c), (d) and Figure 4.2(c), (d) clearly show pores within the composite, which may be formed while APTMS quickly reacts with RF gel. Some of spherical silica/RF composite beads still remain visible (Figure 4.1(d), Figure 4.2(c)) while others left the composite forming into spherical holes (Figure 4.1(c), Figure 4.2(d)). According to Figure 4.3, EDX micrograph shows that silicon is dispersed in all of spherical beads which confirms that all of these beads are silica/RF composite.

Nevertheless, according to the result from BET analysis, the surface area is decreased with the decreasing reaction temperature. The sample formed at room temperature yielded the highest surface area even though it contained the lowest fraction of silica. According to preliminary experiments, it was found that pyrolyzed product of RF gel aged at 0°C had surface area of ~350 m²/g for both drying process. After introduction of APTMS in RF gel, the surface area was decreased. That means APTMS affects wall structure of the pores that results in lesser surface area and total pore volume. So, with decreasing temperature, although increasing of silica content can be achieved, the structure of the pores in the composite is more vulnerable.

Table 4.1 Properties silica/RF composite formed with RF gel that had been aged for 6 h at 0, 5, 10, and 25°C before being added with APTMS.

Aging temperature (°C)	Fraction of APTMS added* (%mol)	Si/C molar ratio	Surface area of pyrolyzed gel (m ² /g)	
			Air dry	Freeze dry
0	2.82	0.028	9.47	208.51
5	2.72	0.027	162.69	195.69
10	2.66	0.026	145.27	108.38
25	2.58	0.026	255.31	244.13

* The fraction of APTMS added was compared to the volume of RF gel being added. The data reported are maximum amount of APTMS that could be added to RF gel.

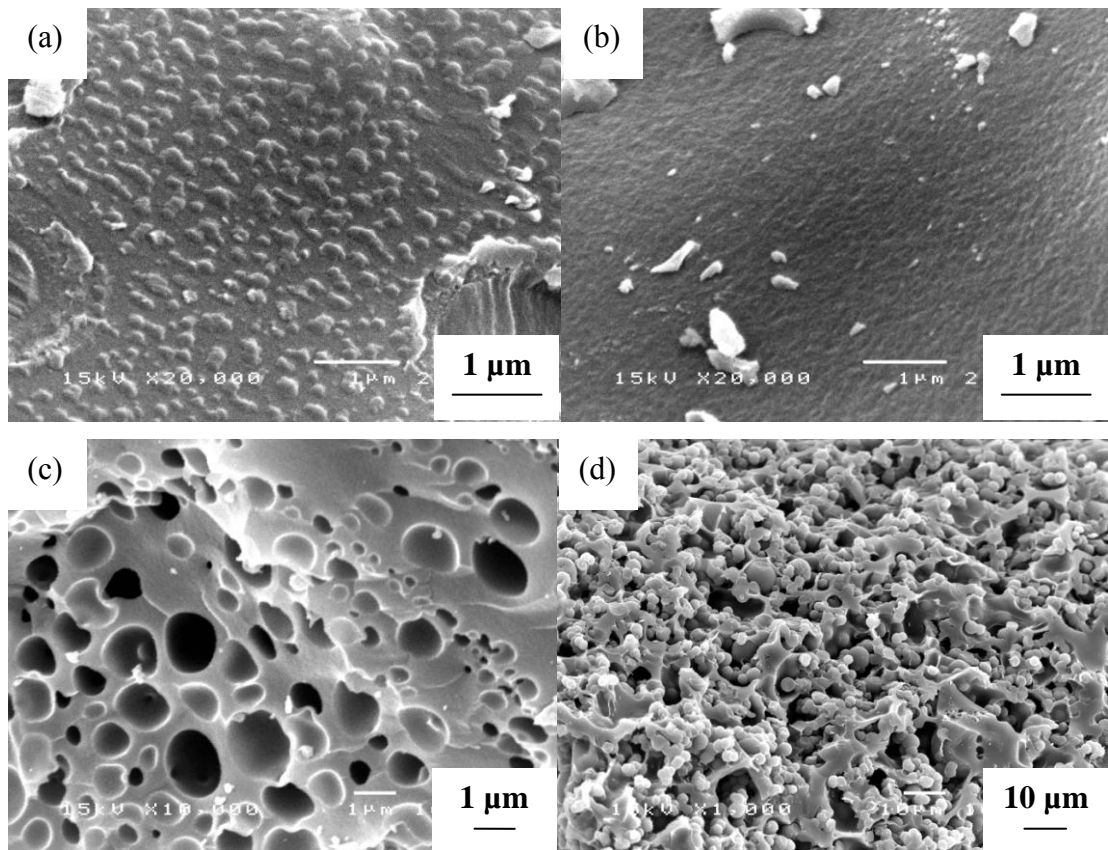


Figure 4.1: SEM micrographs of pyrolyzed silica/RF composites that were dried using convectional drying process. The composites were prepared by using RF gel that had been aged at 0°C (a), 5°C (b), 10°C (c) and 25°C (d) before being added with APTMS.

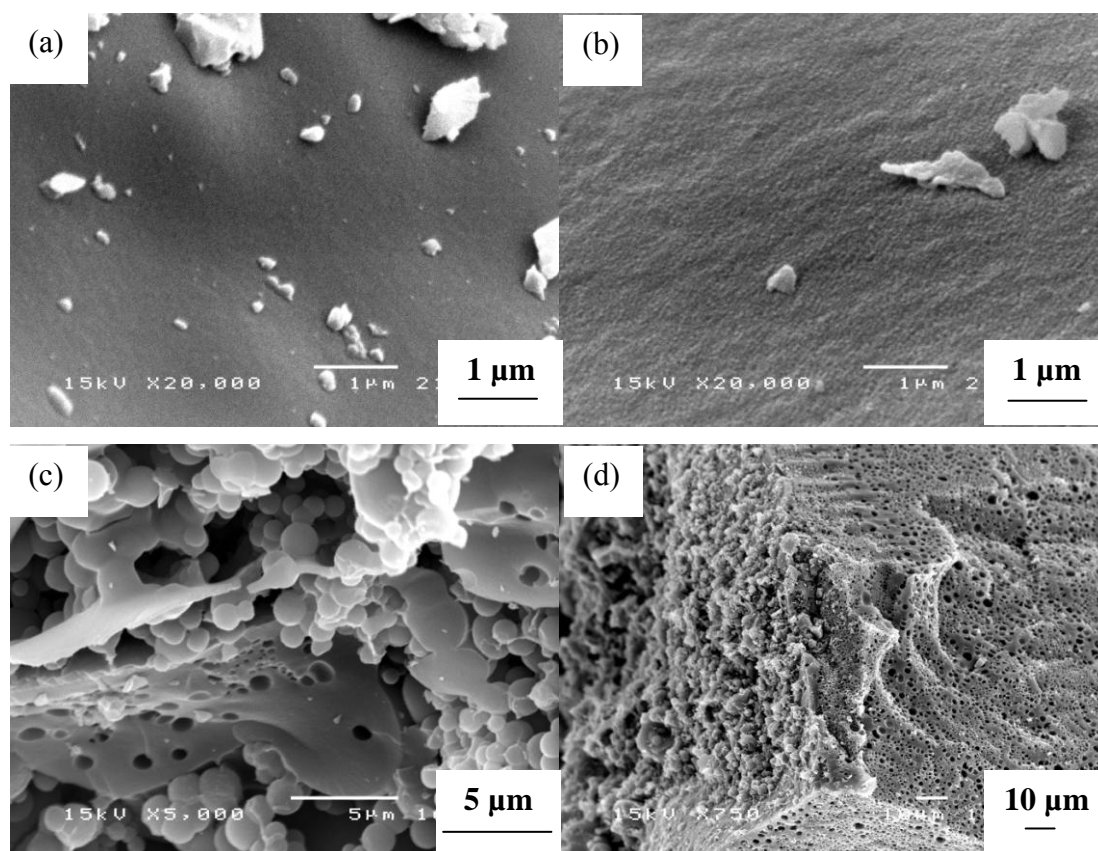


Figure 4.2: SEM micrographs of pyrolyzed silica/RF composites that were dried using freeze drying process. The composites were prepared by using RF gel that had been aged at 0°C (a), 5°C (b), 10°C (c) and 25°C (d) before being added with APTMS.

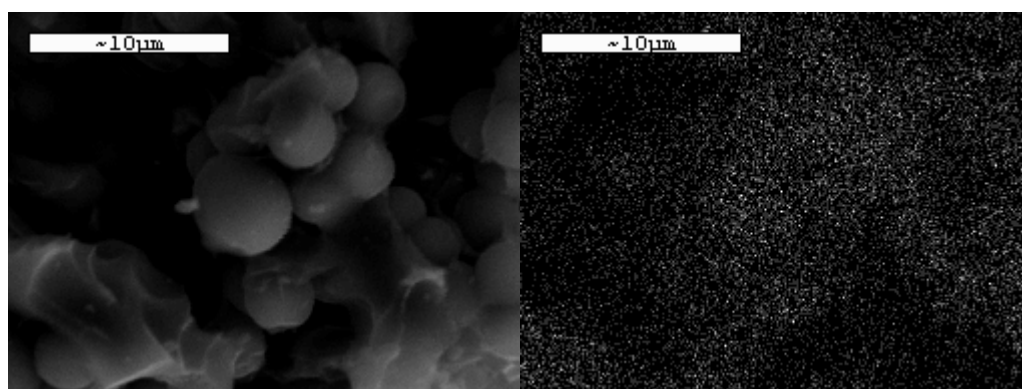


Figure 4.3: EDX mapping for silicon in form of spherical bead particles of pyrolyzed silica/RF composites.

4.1.2 Properties of nitrated products

Selected pyrolyzed samples that yielded maximum silica content and maximum surface area, i.e. the samples prepared at 0°C and 25°C and being dried by freeze drying process, were subjected to the nitridation process. The pyrolyzed samples in each condition were separated into two parts, i.e., powder and solid specimen. For the powder form, the pyrolyzed samples were crushed into the powder before nitridation. Figure 4.4 shows the XRD patterns of the products after nitridation. α -Silicon nitride was obtained only from the sample prepared at 25°C, while β -silicon carbide appeared from both of samples. Since these patterns were obtained from the products after nitridation, it is possible that the broad peak in the XRD patterns is the result from the residual carbon in the products. It is generally considered that SiC is formed by the reaction of silicon monoxide (SiO) vapor with either carbon monoxide (CO) or carbon (C) in the carbothermal reduction process.

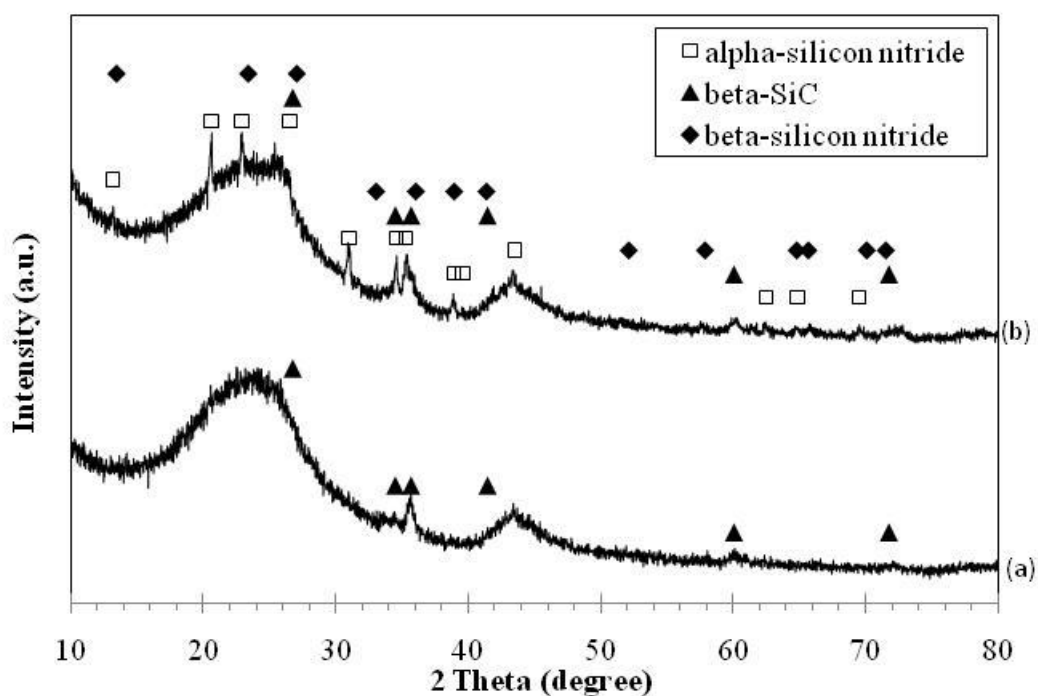
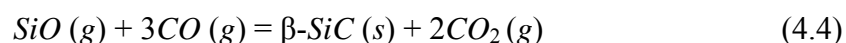
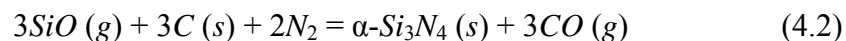


Figure 4.4: XRD patterns of the nitrated products prepared from RF gel aged at 0°C (a) and 25°C (b) without using acetic acid. The composite was freeze-dried before the pyrolysis and subsequent nitridation.

First, SiO₂ was reduced into SiO vapor by active carbons while SiO vaporized out of the pellets (reaction 4.1). Then the nuclei of α-Si₃N₄ were formed through Reaction (4.2). Some of SiO reacted with carbon to form SiC and CO according to Reaction (4.3) followed by further reaction between SiO and produced CO to form SiC and CO₂ via Reaction (4.4). That means the SiO₂/C composite can produce both α-Si₃N₄ and SiC. However, with the less content of carbon, the production of SiC is more favored than α-Si₃N₄. The favorable condition of the formation of SiC is when the partial pressure of CO is greater than 0.027 MPa and the temperature is higher than 1300°C [48]. Jin et al. studied the reaction condition at 1250°C under argon flow. It was found that SiC was mainly produced by the reaction of SiO and carbon. So, it is possible that SiC detected in this research was produced during the heating up of the reactor. However, for the sample prepared at 0°C, which had the maximum silica content, only SiC was obtained. It may be caused by high C/SiO₂ molar ratio. With the increasing of C/SiO₂ molar ratio, the amount of SiC increased sharply [49-51]. The product also contained amorphous phase as the result of XRD analysis in Figure 4.4. It may be caused by un-reacted silica precursor in the composite reacted with N₂ and H₂ directly to form Si-H and N-H bonds which consequently formed into a-SiN_x (amorphous silicon nitride) [52, 53].



Results of TGA analysis in oxygen atmosphere of the nitrated products is shown in Figure 4.5. It can be seen that there was approximately 20 wt% of final products (i.e., Si_3N_4 and SiC) in the composites. The rest was residual carbon. Figure 4.6 suggests that the residual carbon was removed by the calcination process completely since both calcined samples revealed no significant mass decrease during the TGA analysis. Only small amount of moisture, unreacted formaldehyde and t-butanol (the formaldehyde solution is stabilized by alcohol such as methanol and is completely oxidized at 200°C [38, 54]) in the product after calcination was observed. The sample prepared at 0°C showed slightly higher mass loss, after being calcined, than the sample prepared at 25°C . It means that the content of carbon residual in the sample prepared at 0°C is higher than that prepared at 25°C . It should be noted that slight mass increase was observed at the analysis temperature higher than 700°C . This is the result from surface oxidation to form SiO_2 .

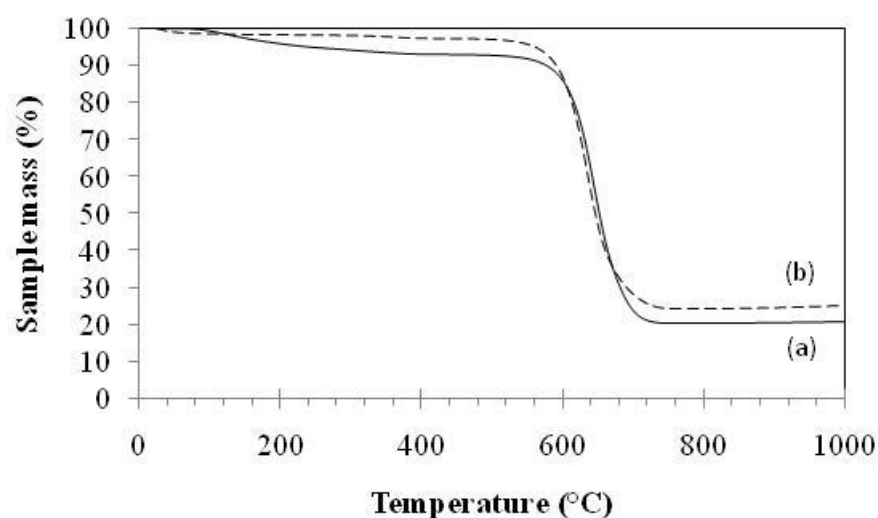


Figure 4.5: Results of TGA analysis in oxygen atmosphere of the nitrated products prepared from RF gel aged at 0°C (a) and 25°C (b) without using acetic acid. The composite was freeze-dried before the pyrolysis and subsequent nitridation.

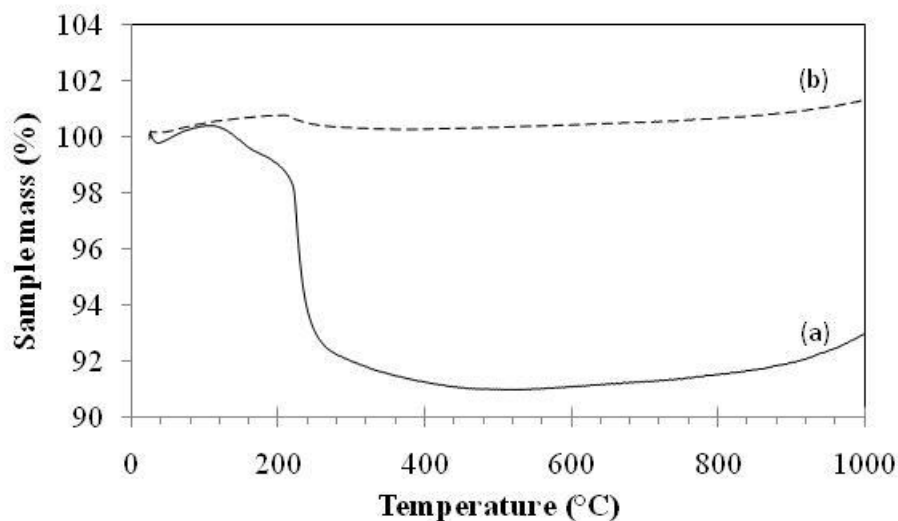


Figure 4.6: Results of TGA analysis in oxygen atmosphere of the calcined nitrated products prepared from RF gel aged at 0°C (a) and 25°C (b) without using acetic acid. The composite was freeze-dried before the pyrolysis and subsequent nitridation.

Table 4.2 presents BET surface area and pore properties of the final products after calcination. BET surface area of the calcined product, prepared at 0°C, (341.65 m²/g) was still high comparing to the pyrolyzed sample (208.51 m²/g). Comparing between powder and solid specimen, the solid sample had lower surface area. It was indicated that diffusion of H₂ and N₂ to react with silica and carbon within the composite in the powder form was easier than that in the form of solid piece. Nevertheless, both products had high surface area and contained mesoporosity. For the sample prepared at 25°C, the sample obtained after nitridation and calcination had smaller surface area (149.48 m²/g) than the sample after pyrolysis (244 m²/g). It should be noted that the TGA results of samples after calcination confirmed the complete removal of carbon from the products. Therefore, the surface area measured belonged to the Si₃N₄ and SiC products, not to the residual carbon.

Table 4.2 Surface area and pore properties of the nitrided products after calcination.

The composite was prepared from RF gel aged at various temperatures without using acetic acid and subjected to freeze drying before being pyrolyzed and subsequently nitrided. The samples were divided into 2 parts, i.e. crushed powder and solid specimen before subjected to the nitridation process.

Temperature (°C)	Surface area (m ² /g)		Pore diameter (nm)		Pore volume (cm ³ /g)	
	Powder	Solid specimen	Powder	Solid specimen	Powder	Solid specimen
0	341.65	238.66	8.82	8.94	0.753	0.533
25	149.48	100.56	2.67	2.46	0.100	0.062

4.2 *Effect of acetic acid*

In this part, various amount of acetic acid was added to 8.83 ml of RF gel to retard interaction between RF gel and APTMS. Maximum amount of APTMS that could be added to the RF gel before the mixture solidified was determined.

4.2.1 Properties of pyrolyzed gel

It can be seen from Table 4.3 that acetic acid showed inhibiting effect toward the reaction between APTMS and RF gel. The maximum amount of APTMS that could be added to RF gel increased as more acetic acid was added to RF gel prior to the addition of APTMS. It was suggested that acetic acid broke cross-linking network within the RF gel, which prolonged the gelation time of the composite, as well as capped the reactive functional group of the RF gel to inhibit reaction with APTMS [38]. Nevertheless, it could be seen that the solid structure of the composite became denser as more acetic acid was added to the RF gel, as shown in Figure 4.7. The lower pH value was, the smaller of dissociated carboxyl groups became which makes the gel a less anionic polyelectrolyte. It is to be expected that the less anionic chains aggregate with one another more easily because of the lower electrostatic repulsion. The ease of aggregation caused by decreasing the pH explains why the structure became densely linked [55, 56].

Table 4.3 Maximum amount of APTMS that could be added to RF gel, based on volume of the RF gel, as a function of acetic acid content in the RF gel.

Fraction of acetic acid (%mol)	Fraction of APTMS (%mol)	Si/C molar ratio	pH value after adding acetic acid
1.25	3.46	0.03	5
2.47	4.16	0.04	4
3.65	4.75	0.04	4
4.81	5.50	0.05	3
5.94	5.87	0.05	3

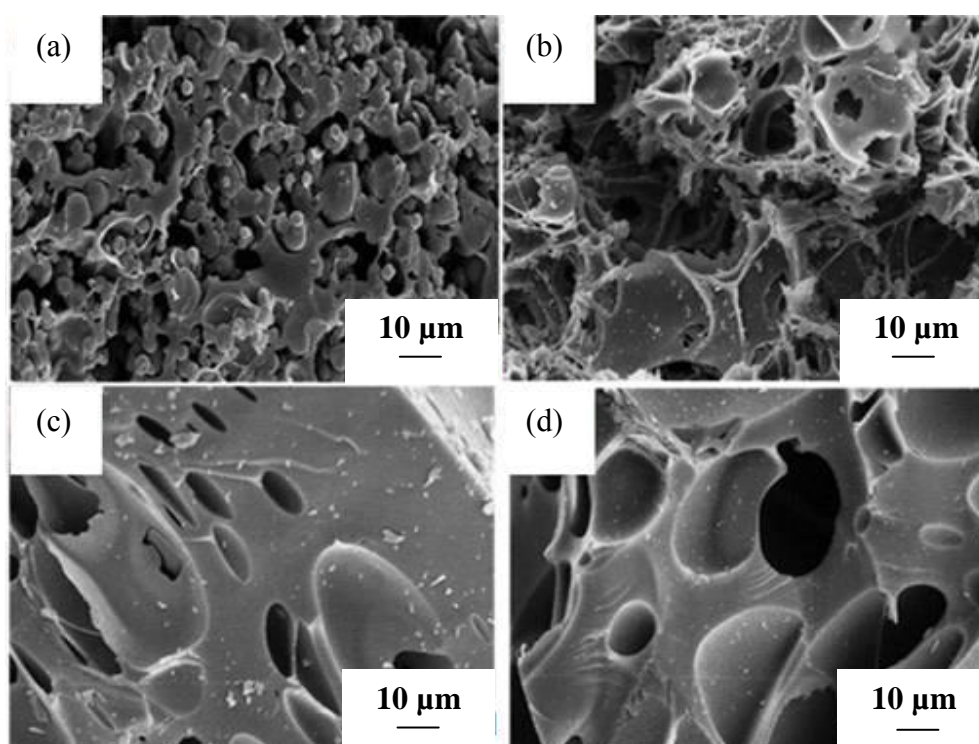


Figure 4.7: SEM micrographs of pyrolyzed silica/RF composites that were dried using convectional drying. The composites were prepared by using RF gel added with acetic acid in the amount of 0 (a), 24.01 (b), 30.67 (c) and 36.26 %mol (d). The gel was formed at room temperature.

Even though addition of acetic acid makes the specimen become denser, it is necessary because, without acetic acid, the composite is fragile. That is a result of less silica content. The use of acetic acid with RF gel that had been aged at low temperature could avoid excessive use of acetic acid, hence resulted in products that were still porous. Acetic acid in the amount corresponding to 5.94 %mol was added to the RF gel aged at various temperatures (i.e., 0°C, 5°C, 10°C, 25°C) to study the effects on the composite. As shown in Figure 4.8 and Figure 4.9, it was found that the obtained composites were still porous. So, acetic acid in the range of 1.25-5.94 %mol was chosen to investigate further in this research. It should be noted that the experiments were done at 0°C to avoid violent reaction with APTMS.

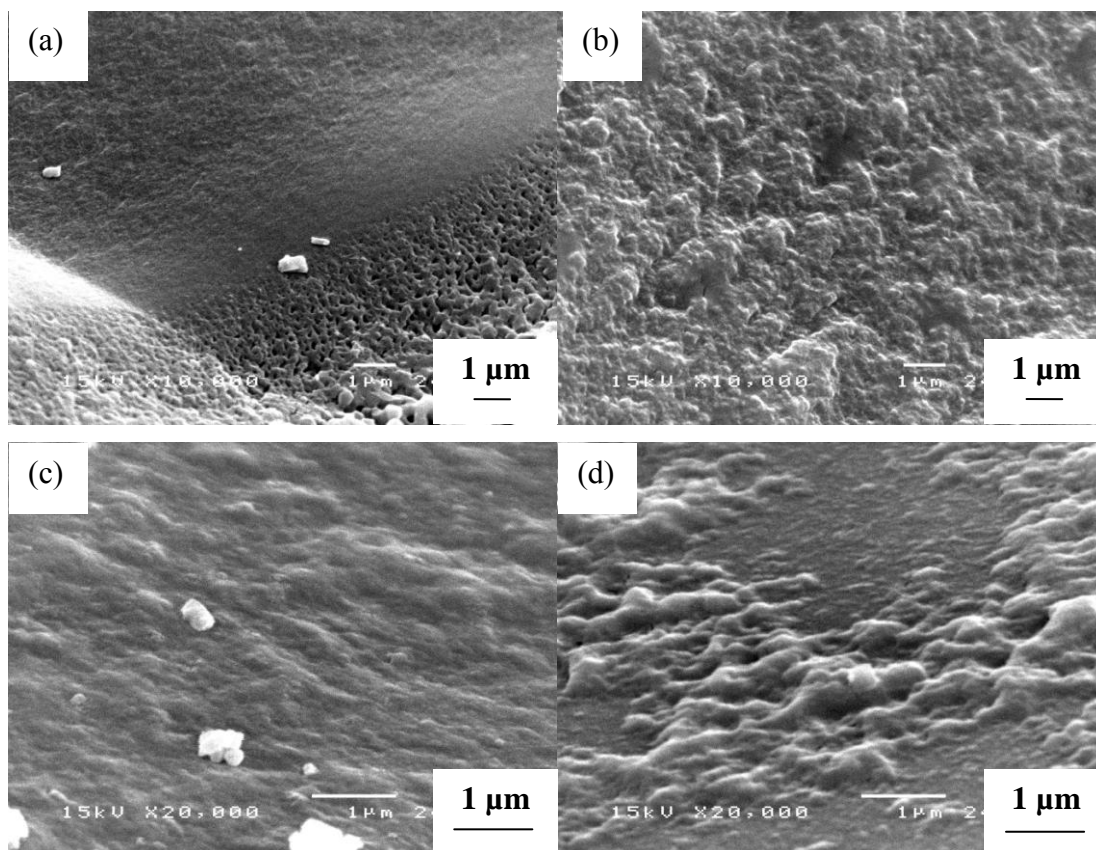


Figure 4.8: SEM micrographs of pyrolyzed silica/RF composites that were dried using convectional drying process. The composites were prepared by using RF gel added with acetic acid in the amount of 5.94 %mol. The gel was formed at 0°C (a), 5°C (b), 10°C (c) and 25°C (d).

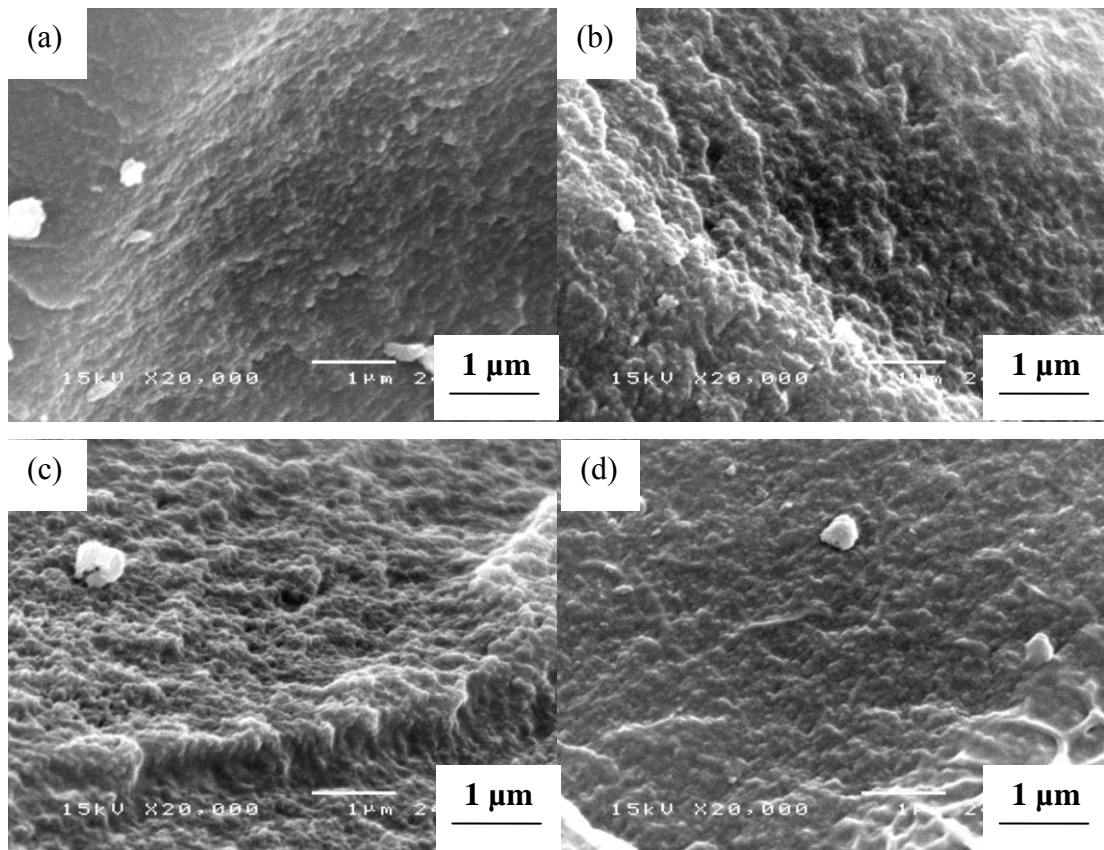


Figure 4.9: SEM micrographs of pyrolyzed silica/RF composites that were dried using freeze drying process. The composites were prepared by using RF gel added with acetic acid in the amount of 5.94 %mol. The gel was formed at 0°C (a), 5°C (b), 10°C (c) and 25°C (d).

Table 4.4 Surface area and pore properties of silica/carbon composite prepared by using various amount of acetic acid. The gel was aged at 0°C before being added with APTMS.

Fraction of acetic acid (%mol)	Convictional air drying			Freeze drying		
	Surface area (m ² /g)	Pore diameter (nm)	Pore volume (cm ³ /g)	Surface area (m ² /g)	Pore diameter (nm)	Pore volume (cm ³ /g)
1.25	3.84	8.72	0.008	2.86	8.17	0.01
2.47	111.00	2.30	0.072	302.29	2.57	0.19
3.65	78.29	2.48	0.047	73.05	2.85	0.06
4.81	12.48	2.65	0.007	1.56	7.28	0.01
5.94	4.35	7.50	0.008	12.18	13.01	0.04

Table 4.4 shows pore properties and surface area of the pyrolyzed composite formed by using different content of acetic acid. It was presented that using low content of acetic acid of 1.25 %mol resulted in product with low surface area and large pore diameter corresponded to the reported by Lin et al. that the decrease in the pH from 6.5 to 5.5 created larger pores which did not contribute much to the surface area [57, 58]. The reaction between silica precursor and RF gel still carried out rapidly and resulted in some of the spherical particles as seen in Figure 4.10(a) and Figure 4.11(a). Although too much of acetic acid into the composite also resulted in non porous material, there was the appropriate amount of acetic acid that could give a composite with high molar ratio of Si/C while having high surface area and high porosity. According to the experimental results, the BET surface area and the total pore volume when the content of acetic acid was 2.47 %mol were the highest. The acetic acid content of 2.47 %mol gave the suitable pH value. Figure 4.10(c, d) and Figure 4.11(c, d) show the smoother surface because of increasing of acetic acid.

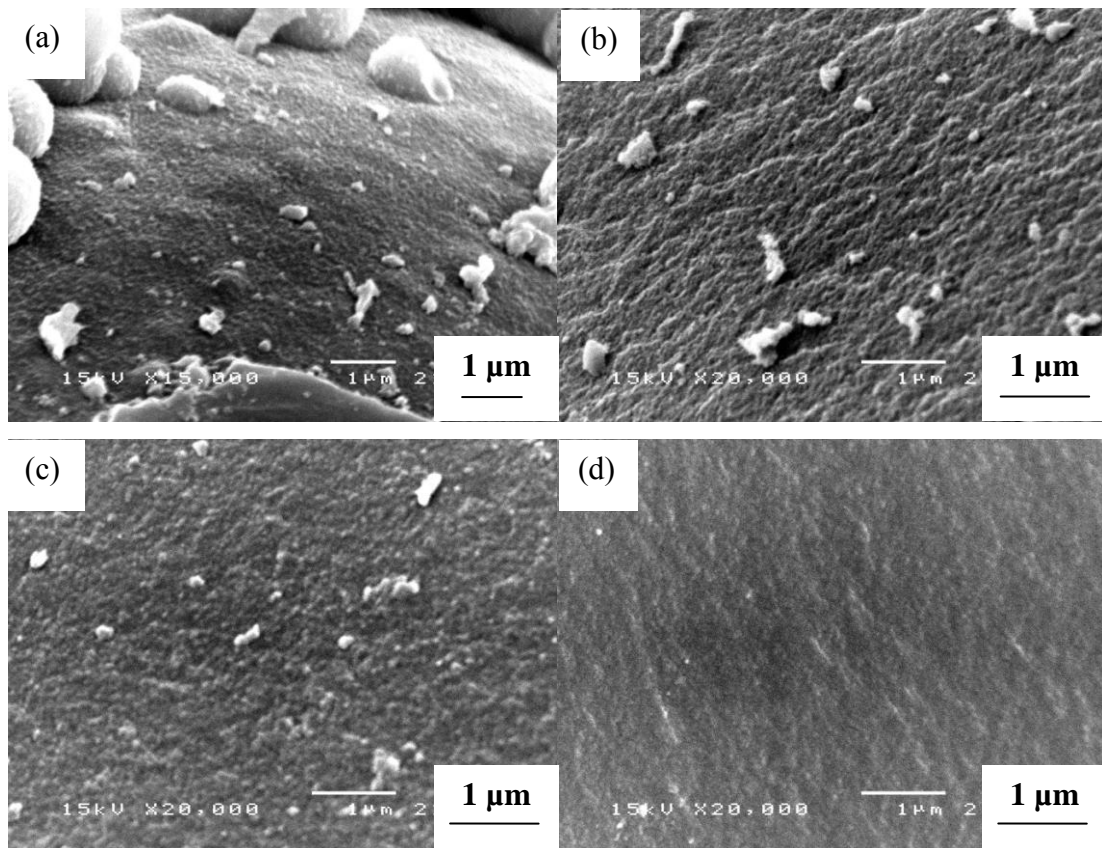


Figure 4.10: SEM micrographs of pyrolyzed silica/RF composites that were dried using convectional drying. The composites were prepared by using RF gel added with acetic acid in the amount of 1.25 (a), 2.47 (b), 3.65 (c) and 4.81 %mol (d).

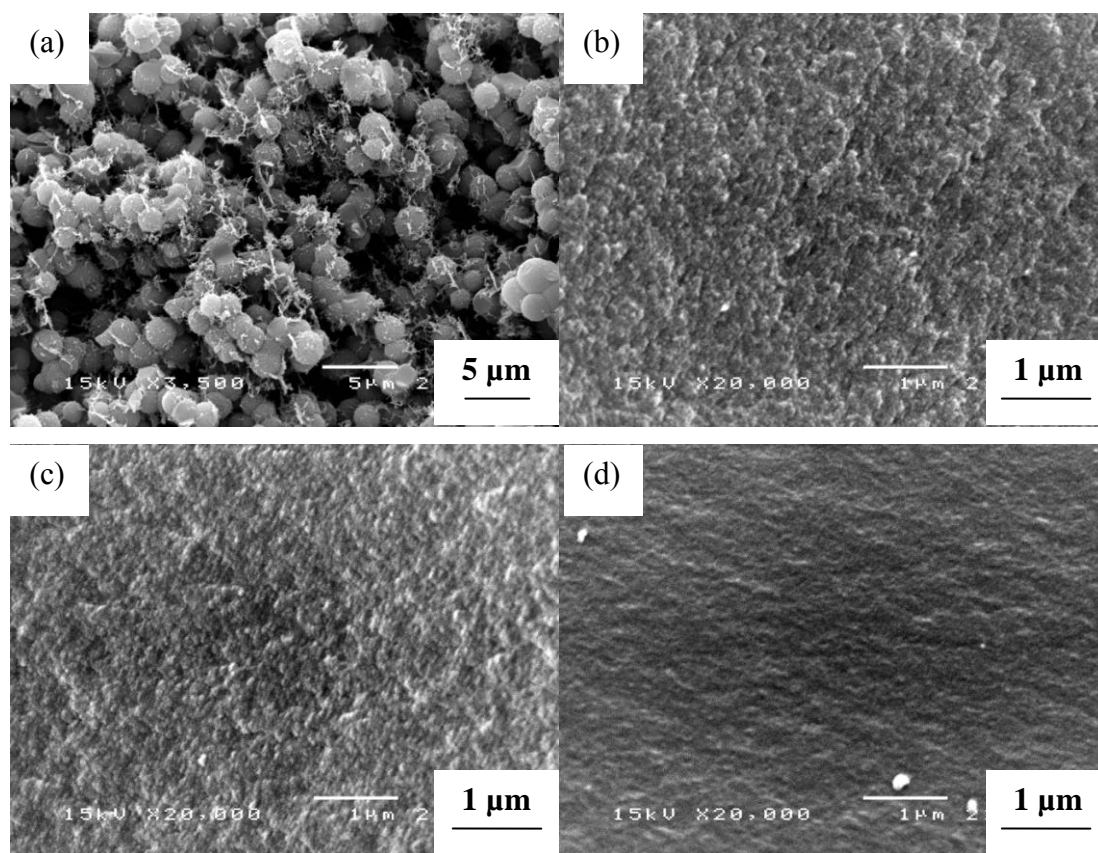


Figure 4.11: SEM micrographs of pyrolyzed silica/RF composites that were dried using freeze drying. The composites were prepared by using RF gel added with acetic acid in the amount of 1.25 (a), 2.47 (b), 3.65 (c) and 4.81 %mol (d).

Figure 4.12 shows FTIR spectra of the gel before being pyrolyzed. By comparing the spectra of samples added with acetic acid to that of the sample without acetic acid, it was found that majority of functional groups detected were similar. The IR absorption bands around 3404 cm^{-1} are corresponding to O-H stretching vibration [59]. A band at 2937 cm^{-1} represents antisymmetric stretching vibration of C-H bonding in methyl groups [34, 59, 60]. The absorption band at 1615 cm^{-1} has been assigned to C=C stretching vibration in aromatic rings [34, 60], while that at 1444 cm^{-1} is C=C bond obscured by $-\text{CH}_2-$ methylene bridge [60]. The IR band at 1102 cm^{-1} corresponds to asymmetric stretching vibration of C-O-C aliphatic ether [60]. These functional groups are associated with RF gel. The presence of silica in the sample was confirmed by the absorption band at wavenumber of 1198 and 696 cm^{-1} , corresponding to antisymmetric and symmetric stretching of Si-O-Si bonding, respectively [59]. The in-plane stretching vibration of Si-OH was also observed around 924 cm^{-1} [59]. The shoulder at wavenumber around 450 cm^{-1} was indicated as the deformation vibration of O-Si-O group [59]. For the samples prepared with the presence of acetic acid, the signal from C=O stretching from unreacted formaldehyde was observed at 1708 cm^{-1} [40]. Even though acetic acid slows the reaction by broken the bond in RF gel, the bonding of methylene bridge and methylene ether bridge were still eventually formed.

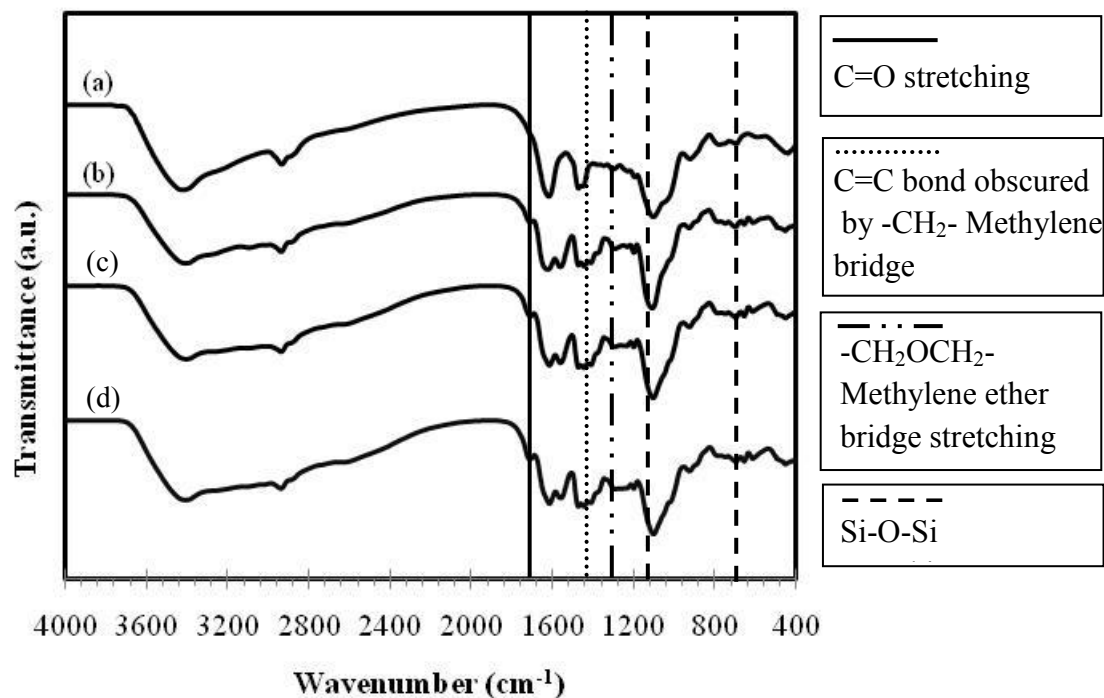


Figure 4.12: FTIR spectra of silica/RF composites prepared by using RF gel with acetic acid content of 0 (a), 24.01 (b), 30.67 (c) and 36.26 %mol (d).

The thermal degradation of the gel formed with the acetic acid content of 2.47 %mol, before and after pyrolysis was investigated and presented in Figure 4.13. The analysis of the dried gel (i.e., before pyrolysis) was conducted in nitrogen atmosphere, which simulated the pyrolysis process that converts silica/RF gel to silica/carbon composite. The sample was heated in the step-wised fasion at 250°C to 750°C similar to that conducted in the pyrolysis. It was found that approximately 50 wt% of organic compound was lost during pyrolysis (Figure 4.13(a)). On the other hand, the analysis of the sample after the pyrolysis was done in the range from 25°C to 1000°C in oxygen atmosphere. The result indicated that there was about 25 wt% of silica in the composite (Figure 4.13(b)).

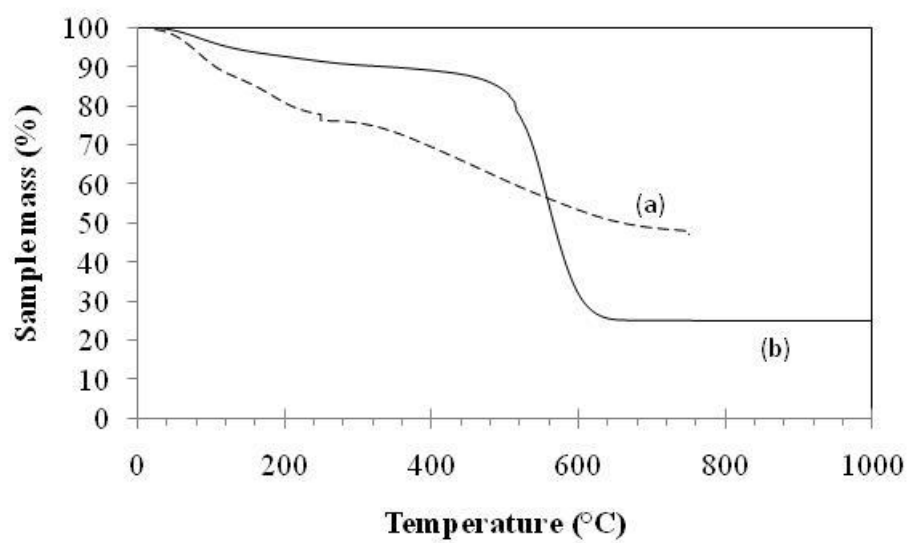


Figure 4.13: Results of TGA analysis of the sample prepared with the acetic acid content of 2.47 %mol, after being freeze-dried (a) and after being pyrolyzed (b).

4.2.2 Properties of nitrated products

The pyrolyzed samples with maximum silica content and maximum surface area were chosen to be further nitrated. In this regard, they were synthesized using the fraction of acetic acid of 5.94 and 2.47 %mol, and being freeze dried, respectively.

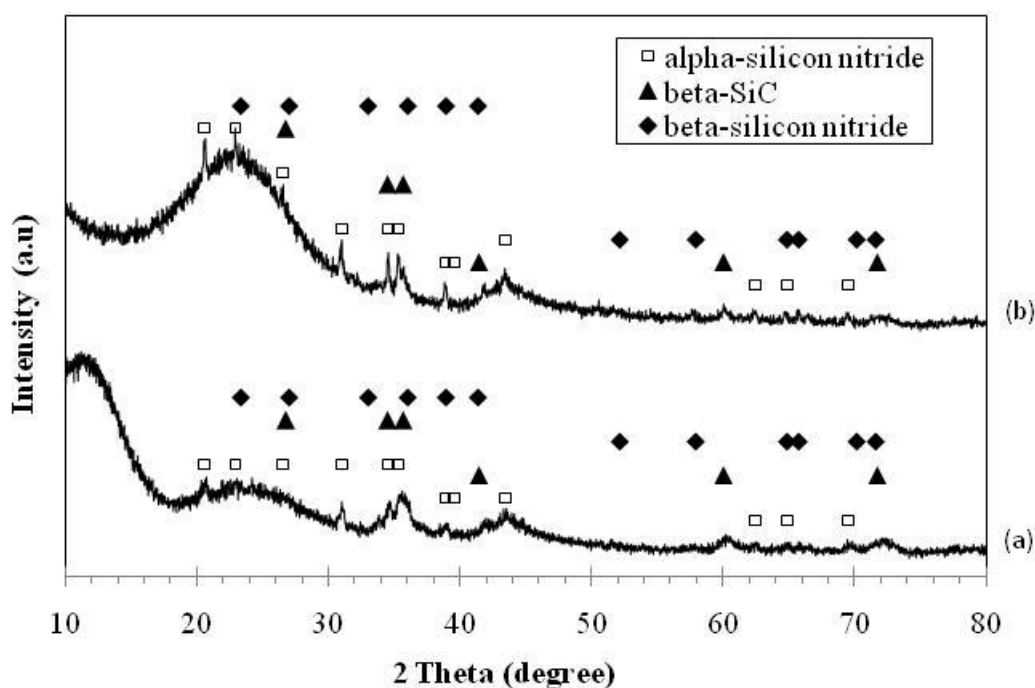


Figure 4.14: XRD patterns of the nitrated products prepared from RF gel using acetic acid content of 2.47 (a) and 5.94 %mol (b). The composite was freeze-dried before the pyrolysis and subsequently nitridation.

The results from the XRD analysis of the final nitrated products are shown in Figure 4.14. It can be seen that addition of acetic acid, which allows more silica to be added to the RF gel, does not affect the formation of silicon nitride. However, broad peaks suggest the presence of phase in the product which may be the result from unreact silica in the composite. The surface areas of the final products after calcination to remove residual carbon are shown in Table 4.5. It is noted that the pyrolyzed sample with the highest surface area (i.e., the sample prepared with 2.47 %mol of

acetic acid with the area of 302.29 m²/g) also produced the final product with high surface area, both in the form of powder and solid specimen (260.97 m²/g and 164.46 m²/g respectively). They both were mesoporous. It is suggested that at the pyrolyzed sample, which had high surface area and high porosity, allowed N₂ and H₂ gas to easily diffuse into pores of the composite to react with silica and carbon to form silicon nitride product. On the other hand, the pyrolyzed sample with the highest silica content (i.e., the sample prepared with 5.94 %mol of acetic acid content) produced the final product with increased surface area (166.51 m²/g in powder form and 162.17 m²/g in the form of solid piece) as well, although its initial surface area before the pyrolysis was low (12.18 m²/g). Therefore, high silica content in the composite can increase the surface area of the product. It can be concluded that high porosity in the pyrolyzed samples is important for the production of porous silicon nitride in monolith form.

Table 4.5 Surface area and pore properties of the nitrated products after calcination process. The composite was prepared from RF gel aged at 0°C with using various acetic acid and subjected to freeze drying before being pyrolyzed and subsequently nitrated. The samples were divided into 2 parts, i.e. crushed powder and solid specimens before subjected to the nitridation process.

Fraction of acetic acid (%mol)	SiO ₂ /C molar ratio	Surface area (m ² /g)		Pore diameter (nm)		Pore volume (cm ³ /g)	
		Powder	Solid specimen	Powder	Solid specimen	Powder	Solid specimen
2.47	0.04	260.97	164.46	11.12	13.99	0.726	0.575
5.94	0.05	166.51	162.17	3.55	3.25	0.148	0.131

Results from TGA analysis in oxygen atmosphere of the nitrated products are shown in Figure 4.15. Both products indicated a total weight loss of about 70 wt%, though the sample prepared with the acetic acid content of 5.94 %mol showed a wider range of decomposition temperature (600-800°C) as shown in Figure 4.15(b). It was indicated that the sample was not homogenous. Not all sample was decomposed at all in the temperature of 600°C. Figure 4.16 shows the TGA analysis results of the final products after calcination. It can be seen that residual carbon in the nitrated products was completely removed by the calcination for both samples. Only slight amount of residual carbon (c.a. 4 wt%) remained after calcination. Surface oxidation was observed with both of samples. Samples with higher silica content showed slightly higher degree of oxidation than the sample with lower silica content [20].

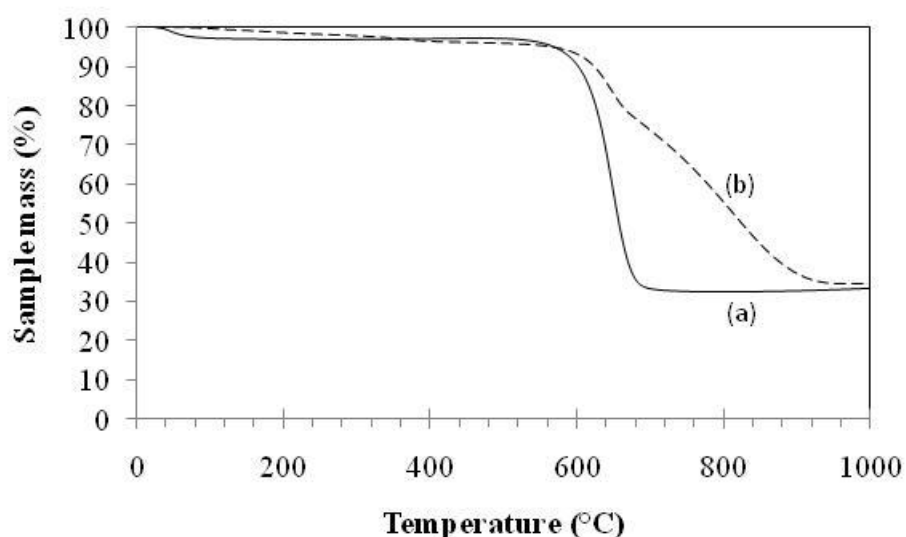


Figure 4.15: Results of TGA analysis in oxygen atmosphere of the nitrated products fabricated from the gel prepared at 0°C, using acetic acid content of: 2.47 (a) and 5.94 %mol (b).

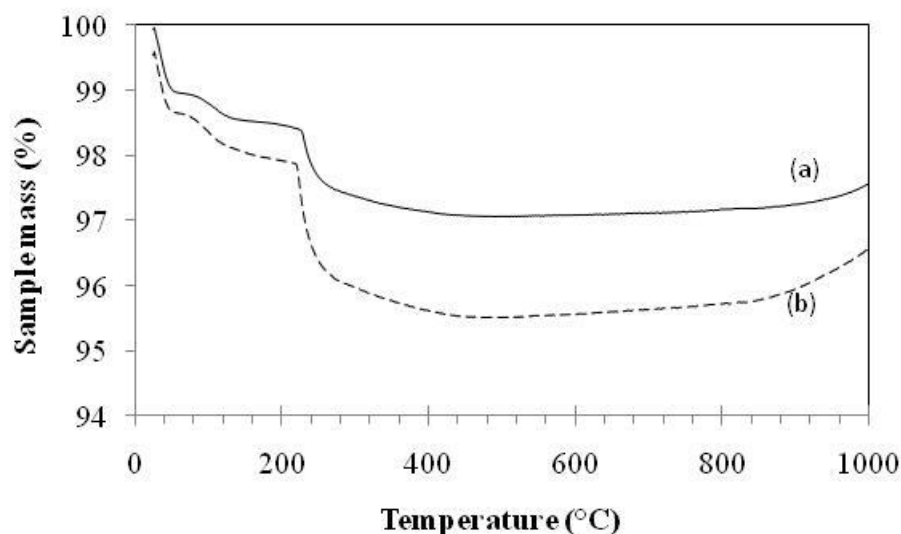


Figure 4.16: Results of TGA analysis in oxygen atmosphere of the final calcined products fabricated from the gel prepared at 0°C, using acetic acid content of: 2.47 (a) and 5.94 %mol (b).

Figure 4.17 and 4.18 show SEM micrographs of the products in the form of solid piece after nitridation, prepared from freeze dried RF gel with acetic acid content of 2.47 and 5.94 %mol, respectively. On the surface of the specimen, as shown in Figure 4.17(a), rod-like structures were formed. It was suggested that carbon reduced SiO_2 , inside the composite, into SiO vapor and then diffused outward to the surface to react with N_2 . The Si_3N_4 was formed at the surface and acted as seeds. After that, SiO which continued diffusing outward and the supplied N_2 reacted on Si_3N_4 seeds via the vapor-solid mechanism. The rod-whiskers were grown on Si_3N_4 at the surface. In the center of the specimen (Figure 4.17(b)), it can be observed that there was rough grain structure. It may be caused by Si_3N_4 formed inside the specimen in similar manner as mentioned above. However, the size of the whisker was bigger than the pore diameter so that, it could not grow bigger. Similarly, in Figure 4.18, combination of spherical and rod-like structures was also observed in the center of the specimen prepared with acetic acid content of 5.94 %mol.

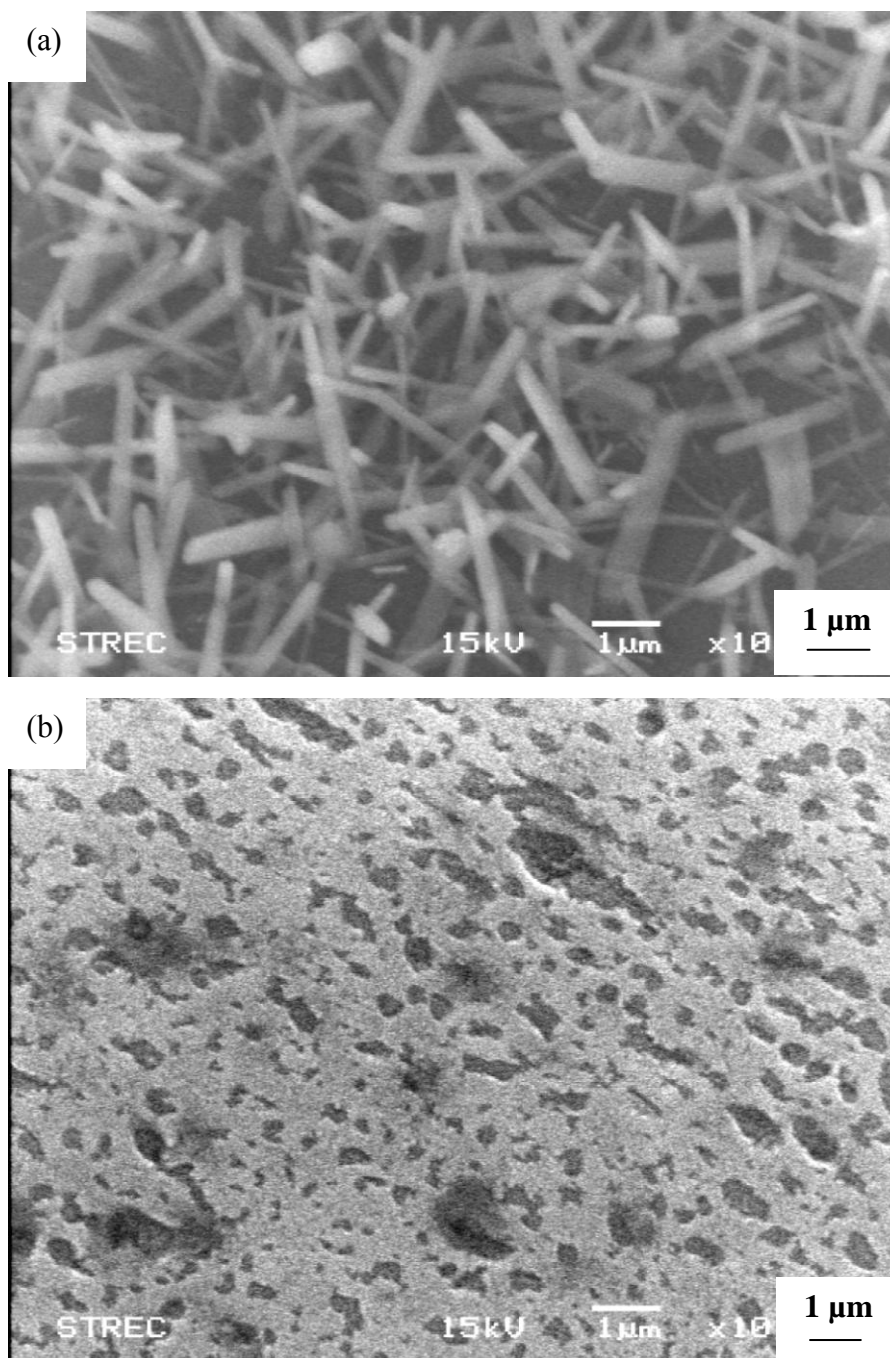


Figure 4.17: SEM micrographs of the nitrided product in the form of solid piece, prepared from RF gel with acetic acid content of 2.47 %mol. The micrographs were taken at the surface (a) and in the center (b) of the specimen.

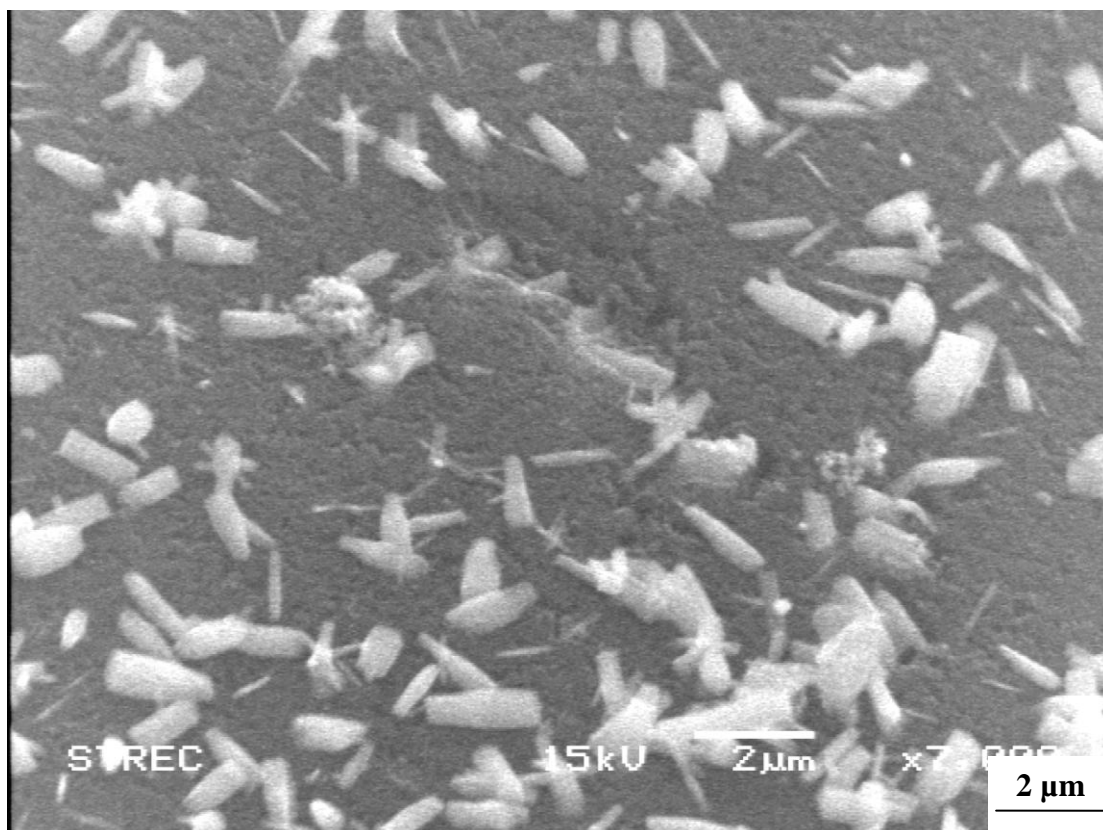


Figure 4.18: SEM micrographs of the nitrided product in the form of solid piece, prepared from RF gel with acetic acid content of 5.94 %mol. The micrographs were taken in the center of the specimen.

4.3 *Effect of drying process*

In this section, effects of different drying technique (i.e., convectonal air drying and freeze drying) are investigated.

4.3.1 Properties of pyrolyzed gel

According to data in Table 4.4 which are also plotted as shown in Figure 4.19 and 4.20, samples that were subjected to freeze drying process had a higher surface area and total pore volume than those dried conventionally. In freeze drying process, solvent inside the pores was frozen and no capillary force acted on the pore wall, hence porous structure could be effectively retained. On the other hand, during convectonal drying, capillary force occurred on the gas-liquid interface. Total pore volume of the sample prepared with convectonal drying was lower than that sample with freeze drying because the pore of carbon was decreased by shrinkage of collapsed structure during pyrolysis (see in Figure 4.20) [37]. From Figure 4.21 and Figure 4.22, it was represented that both drying processes produced the composite with mesopore and micropores. Freeze drying could produce more mesoporosity than the convectonal air drying.

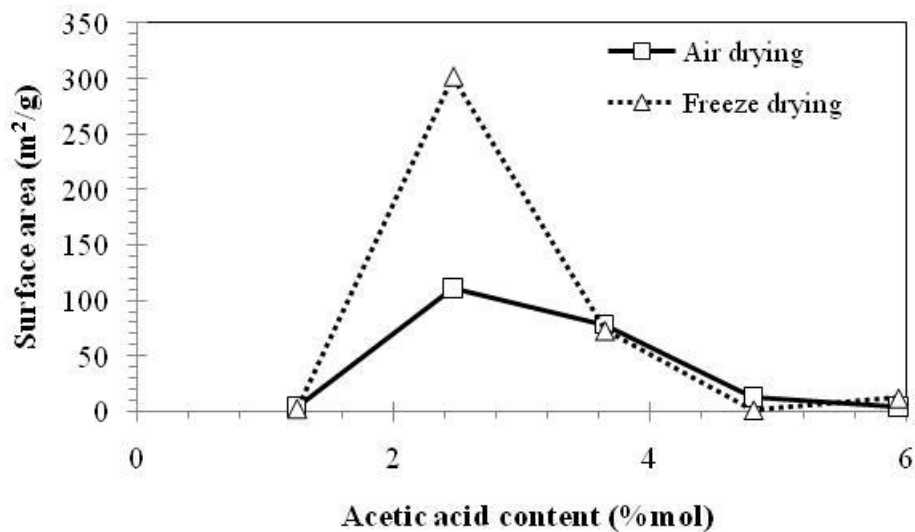


Figure 4.19: Relationship between the content of acetic acid and surface area of silica/carbon composite prepared by using different drying process.

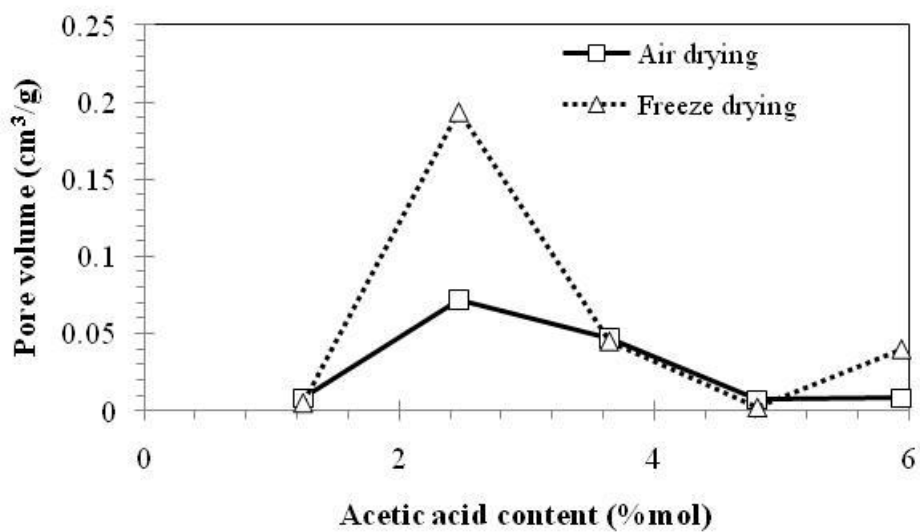


Figure 4.20: Relationship between the content of acetic acid and pore volume of silica/carbon composite prepared by using different drying process.

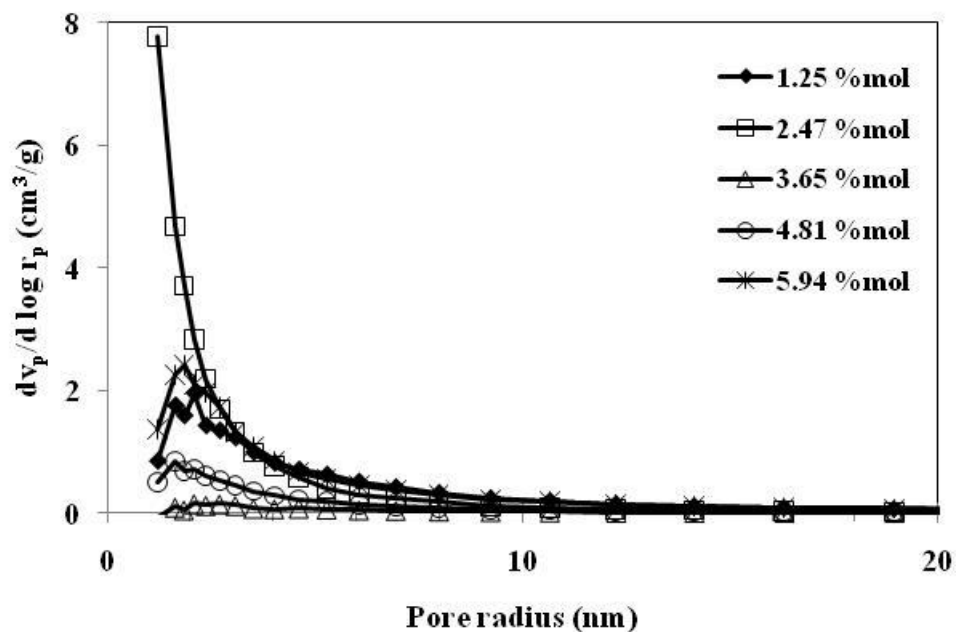


Figure 4.21: Pore size distribution of silica/carbon composite prepared by using different acetic acid content. The composites were dried by convectional drying process.

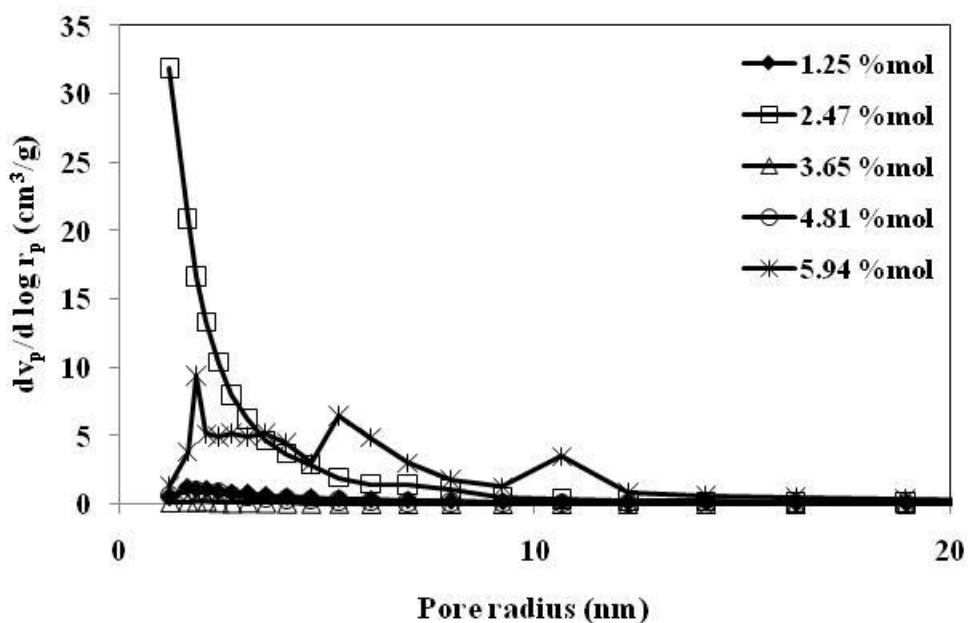


Figure 4.22: Pore size distribution of silica/carbon composite prepared by using different acetic acid content. The composites were dried by freeze drying process.

4.3.2 Properties of nitrated products

The sample prepared by the RF gel aged at 25°C without using acetic acid was chosen to study the effect of drying process toward properties of the nitrated product. XRD patterns of the obtained products, prepared with different drying process, are shown in Figure 4.23. It is indicated that drying process has no effect toward the phase of the product. Drying process only affected porosity and surface area of the product.

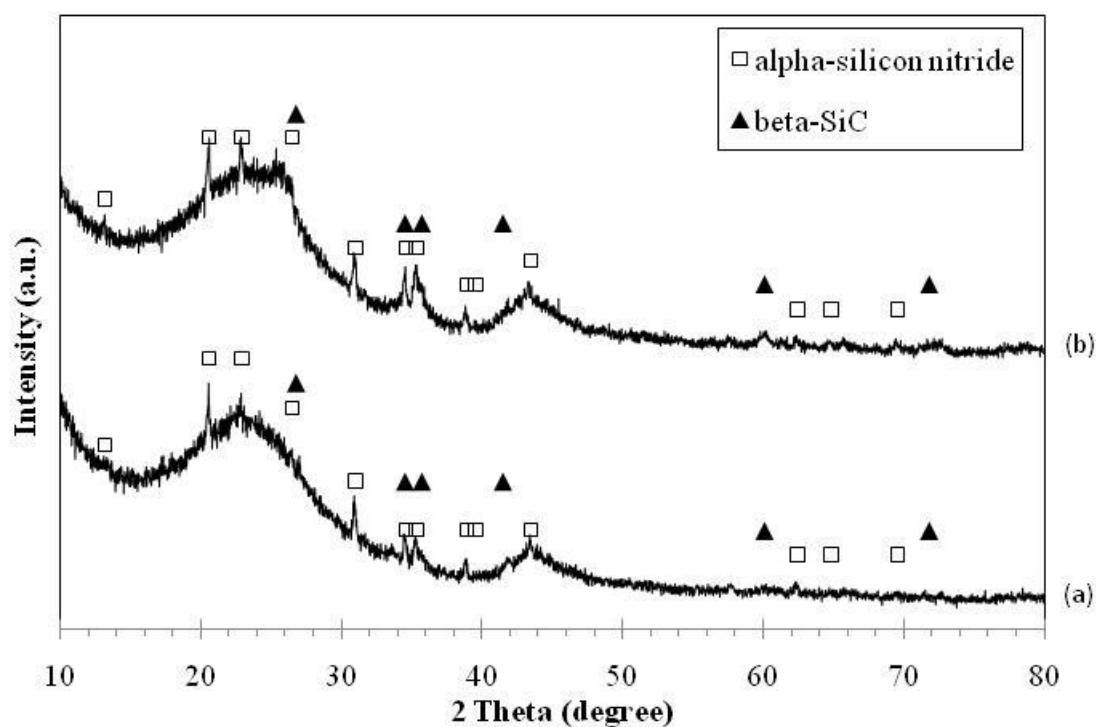


Figure 4.23: XRD patterns of the nitrated products prepared from RF gel without using acetic acid. The composites were prepared by convectional (a) and freeze-drying (b) process.

According to the BET results in Table 4.1, the pyrolyzed gel still had relatively high surface area. Regardless of the drying process, i.e., 255.31 m²/g for the pyrolyzed sample prepared with convectional air drying and 244.13 m²/g for that prepared by freeze drying.

After nitridation and calcination processes, the pore size and surface area of the samples were measured as presented in Table 4.6. The results show that the surface area of both samples decreased but still remained at relatively high value. Even though convectional drying yielded a slight higher surface area in the sample in powder form than that in solid form, but when compared with the sample in form of solid piece, freeze drying provided higher surface area. It may be caused that the slight higher surface area of pyrolyzed sample with convectional drying results in slight higher of that nitrided sample. It was confirmed that freeze drying enhanced the total pore volume and surface area. Comparing between powder and solid specimen for both drying techniques, the solid sample had lower surface area. It was indicated that diffusion of H₂ and N₂ to react with silica and carbon within the composite in the powder form was easier than that in solid form [61].

Table 4.6 Surface area and pore properties of the nitrided products after calcination process. The composite was prepared from RF gel aged at 25°C without using acetic acid and subjected to various drying before being pyrolyzed and subsequently nitrided. The samples were divided into 2 parts, i.e. crushed powder and solid specimens before subjected to the nitridation process.

Drying Process	Surface area (m ² /g)		Pore diameter (nm)		Pore volume (cm ³ /g)	
	Powder	Solid specimen	Powder	Solid specimen	Powder	Solid specimen
Convectional drying	163.31	89.21	2.463	2.488	0.101	0.056
Freeze drying	149.48	100.56	2.669	2.464	0.100	0.062

Figure 4.24 shows the results from TGA analyses in oxygen atmosphere of nitrated samples prepared by using different drying process. Comparing the samples nitrated in powder form (Figure 4.24(a), and 4.24(c)), the total weight loss of about 75 wt% was found in samples prepared by both drying processes. On the other hand, for samples nitride as solid piece, as shown in Figure 4.24 (b) and (d), the samples prepared with freeze drying showed about 20 wt%. less carbon residue after nitridation than that treated with convectional air drying. It was suggested that freeze drying give the stronger structure than convectional drying because of heat collapsed the structure and resulted in a good monolithic structure, which is already confirmed by higher surface area than that obtained from the solid formed with air convectional drying. The sample nitrated in solid form with convectional drying (see Figure 4.24 (b)) has higher content of residual carbon than that of solid sample dried with freeze drying (see Figure 4.24 (d)). It means that samples nitrated as solid with freeze drying can produce more products (i.e., Si_3N_4 and SiC) and results in higher surface area. Because the more carbon had lost, the more products were formed.

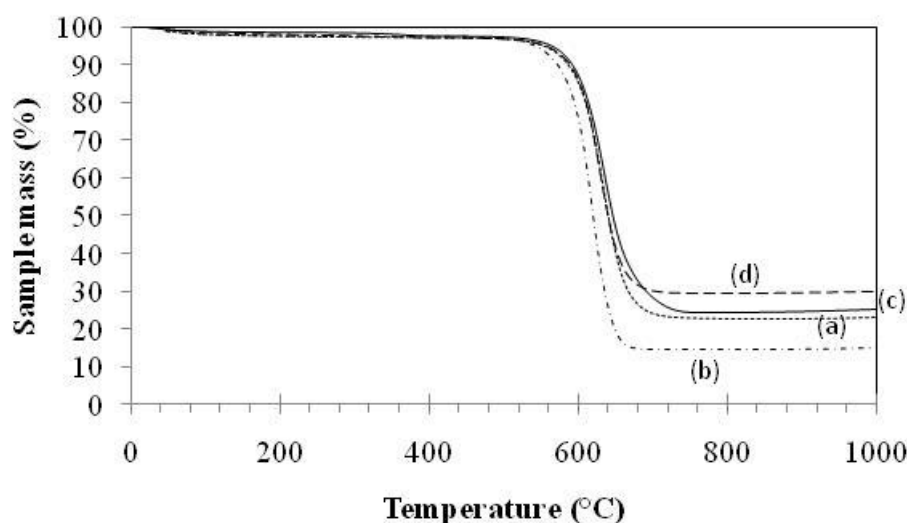


Figure 4.24: Results of TGA analysis in oxygen atmosphere of the nitrided products prepared from RF gel aged at 25°C without using acetic acid. The samples were nitride in different formed: (a) powder prepared by convectional drying, (b) solid piece prepared by convectional drying, (c) powder prepared by freeze drying and (d) solid piece prepared by freeze drying.

Figure 4.25 presents results from TGA analysis in oxygen atmosphere of the nitride products after calcination. The calcination was quite effective in removing residual carbon. Almost no weight loss appeared for all samples. It should be noted that approximately 3 wt% of sample mass loss was detected from the powder sample prepared using convectional drying. Although it was considered very low, it may be caused of moisture content. At the temperature higher than 800°C, slight increases in sample mass were observed due to surface oxidation of silicon nitride.

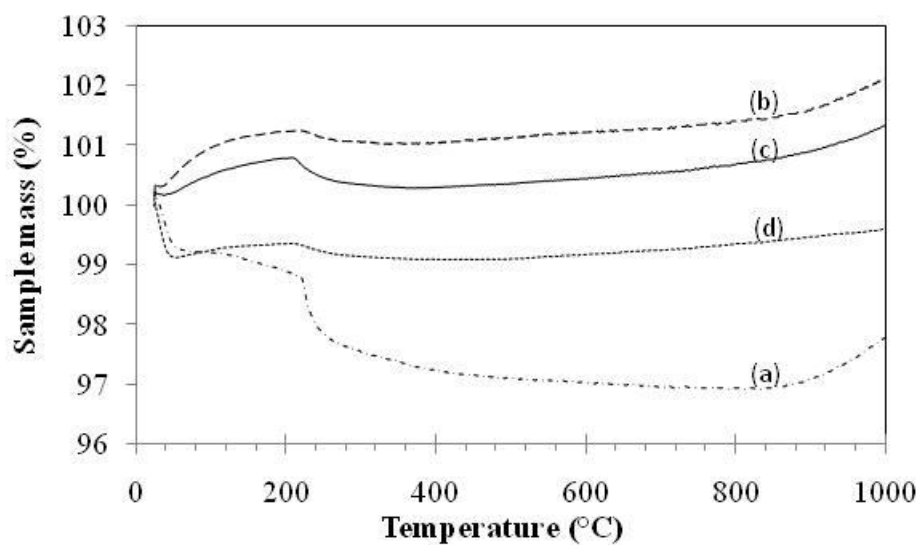


Figure 4.25: Results of TGA analysis in oxygen atmosphere of the calcined nitrated products prepared from RF gel aged at 25°C without using acetic acid. The samples were nitride in different formed: (a) powder prepared by convectional drying, (b) solid piece prepared by convectional drying, (c) powder prepared by freeze drying and (d) solid piece prepared by freeze drying.

4.4 *The use of silica sol as silica source*

In this part, APTMS was left reacting with water and ethanol to form silica sol before being added into RF gel, which had been aged at 0°C for 6 h. This is another way to decrease violent interaction between silica precursor and the RF gel causing an increase in the gel time. Therefore, greater amount of silica could be introduced into RF gel than when fresh APTMS was used. According to the results reported in previous section, the maximum amount of pure APTMS that could be added to the RF gel, prepared with acetic acid content of 5.94 %mol, was 5.87 %mol. When the pre-formed silica sol was used as source, the silica content equivalent to higher amount of APTMS could be introduced to the RF gel as shown in Table 4.7. It should be noted that, if acetic acid was not used, the maximum content of silica that could be added to the RF gel was equivalent to APTMS of 2.82 %mol.

Table 4.7 Composition of silica/RF composite prepared by using pre-formed silica sol as source.

Molar ratio			Fraction of APTMS (%mol)	Si/C molar ratio	Content of acetic acid in RF gel (%mol)	pH of the silica sol-RF mixture
APTMS	Ethanol	Water				
0.13	1.23	1	2.82*	0.04	0	11
0.35	1.23	1	6.21	0.12	5.94	3
0.37	1.23	1	6.56	0.12	5.94	3
0.39	1.23	1	6.90	0.13	5.94	3

4.4.1 Properties of pyrolyzed gel

Table 4.8 shows surface area and pore properties of the pyrolyzed silica/RF composite prepared using silica sol. Even though using pre-formed silica sol allowed higher silica content in the RF gel, but the porosity and surface area of the obtained product were low. It was suggested that the APTMS was first formed into sol with water and ethanol before adding in to the RF gel, resulting in the decrease of violent reaction between APTMS and RF gel. Comparing between the use of APTMS and that of pre-formed silica sol at the content of APTMS of 2.82 %mol, it was found that the use of pre-formed silica sol yielded higher surface area (271.36 and 306.52 m²/g for convectional and freeze drying, respectively) than the use of APTMS (9.47 and 200.51 m²/g for convectional and freeze drying, respectively as seen in Table 4.1).

Table 4.8 Surface area and pore properties of silica/RF composite prepared by using preformed silica sol.

Content of APTMS (%mol)	Convectional air drying			Freeze drying		
	Surface area (m ² /g)	Pore diameter (nm)	Pore volume (cm ³ /g)	Surface area (m ² /g)	Pore diameter (nm)	Pore volume (cm ³ /g)
2.82	271.36	2.3141	0.157	306.52	2.6886	0.206
6.21	14.1580	3.9697	0.0141	33.93	3.3295	0.0282
6.56	1.1939	7.4448	0.0022	0.3839	14.944	0.0014
6.90	1.0507	9.0396	0.0024	6.8761	4.6065	0.0079

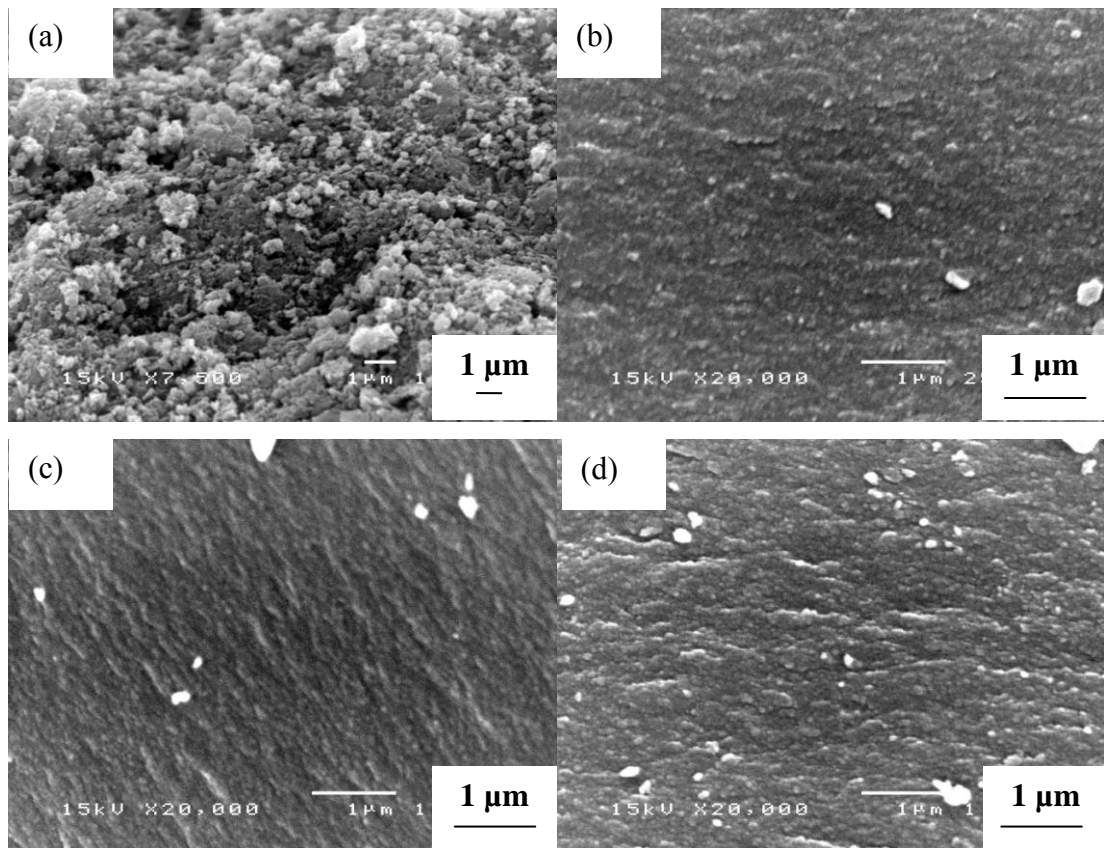


Figure 4.26: SEM micrographs of pyrolyzed pre-formed silica sol/RF composites that were dried using convectional drying. The composites were prepared by using RF with different silica content of 2.82 (a), 6.21 (b), 6.56 (c) and 6.90 %mol (d).

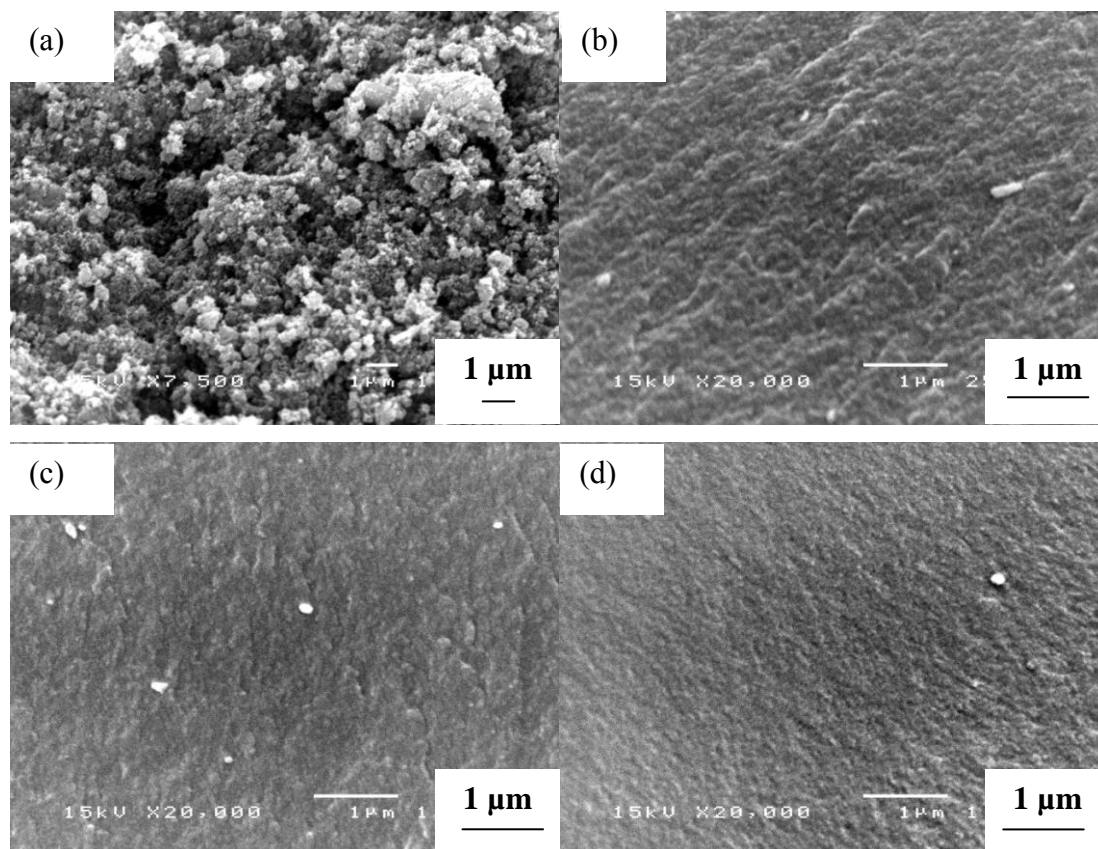


Figure 4.27: SEM micrographs of pyrolyzed pre-formed silica sol/RF composites that were dried using freeze drying. The composites were prepared by using RF with different silica content of 2.82 (a), 6.21 (b), 6.56 (c) and 6.90 %mol (d).

SEM micrographs of pyrolyzed silica/carbon samples, prepared by using pre-formed silica sol at different silica content are shown in Figure 4.26 and Figure 4.27. Figure 4.26(a) and Figure 4.27(a) show the samples, formed without acetic acid, dried by convectional and freeze drying process, respectively. The samples had a quite rough surface. Figure 4.26(b), 4.26(c), 4.26(d), 4.27(b), 4.27(c) and 4.27(d), were the samples with using the acetic acid, show the rough grain surface.

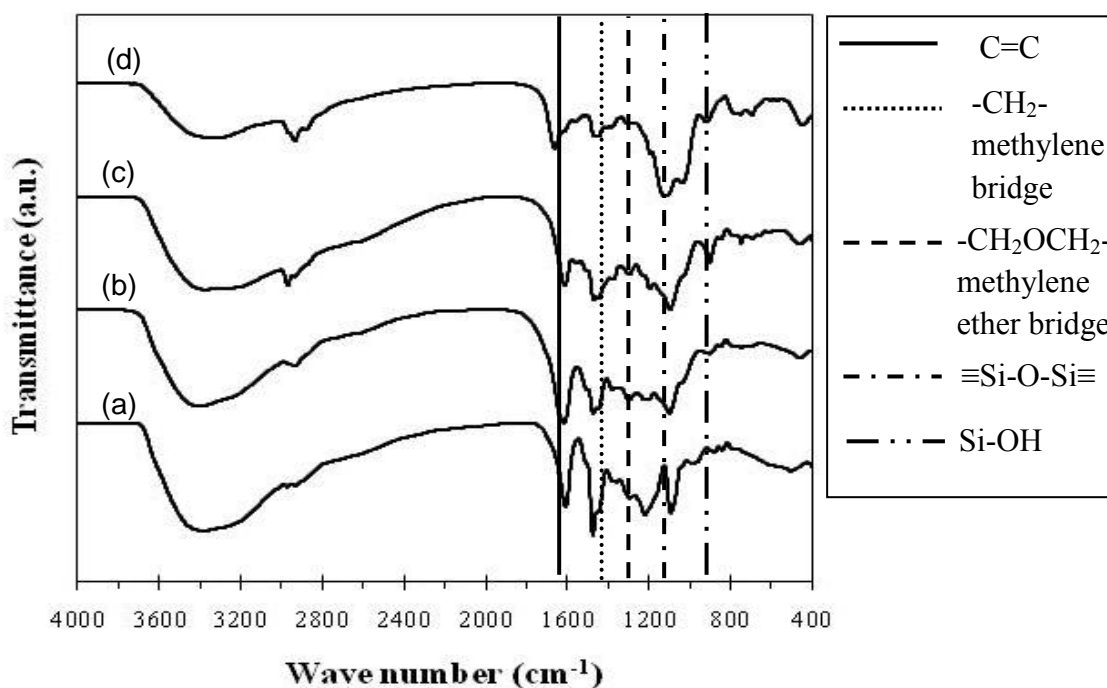


Figure 4.28: FTIR spectra of silica/RF composites prepared by using preformed silica sol with various compositions: (a) RF-EtOH without acetic acid, (b) RF-EtOH-SiO₂ without acetic acid, (c) RF-EtOH-SiO₂ with acetic acid, (d) RF-SiO₂ with acetic acid.

Figure 4.28 showed FTIR spectra of pre-formed silica sol in RF gel that were taken to investigate the effect of functional group by comparing the spectra of samples added with acetic acid and/or ethanol to that of the sample without acetic acid and/or ethanol. It was found that majority of functional groups detected were similar. The IR absorption bands around 3404 cm⁻¹ are corresponding to O-H stretching vibration [59]. A band at 2937 cm⁻¹ represents antisymmetric stretching vibration of C-H bonding in methyl groups [34, 59, 60]. The absorption band at 1615 cm⁻¹ has been assigned to C=C stretching vibration in aromatic rings [34, 60], while that at 1444 cm⁻¹ is C=C bond obscured by -CH₂- methylene bridge [60]. The IR band at 1102 cm⁻¹ corresponds to asymmetric stretching vibration of C-O-C aliphatic ether [60]. These functional groups are associated with RF gel in all of samples. Signals at 1208 and 1088 cm⁻¹ show the antisymmetrical stretching of the ≡Si-O-Si≡ [62]. The

band due to the silanol groups (Si-OH) appears at 925 cm^{-1} [63]. The 801 cm^{-1} and 447 cm^{-1} bands, attribute to the Si-O-Si ring vibration to form three- to four-membered rings [64]. These show that the ethanol has no affect on the bond between RF and silica precursor since the FTIR results which shown that there is no new chemical bonding between RF and silica precursor. The ethanol acted only as reagent in alcoholysis reaction that can be dissolved the silica gel becomes to sol easily for adding into RF gel.

4.4.2 Properties of nitrated products

The samples, with silica content of 2.82 and 6.90 %mol both of which were prepared by freeze drying, were selected to be further nitride because they showed the maximum surface area and maximum silica content, respectively.

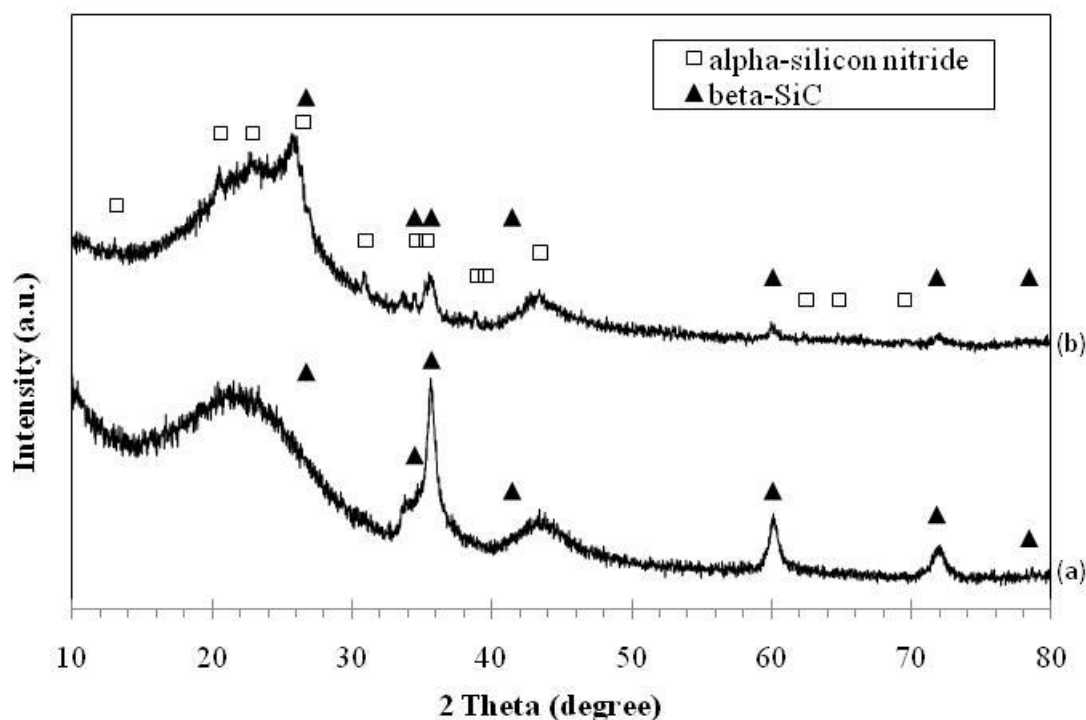


Figure 4.29: XRD patterns of the nitrated products prepared from pre-formed silica sol; 2.82 (a) and 6.90 %mol (b), and RF gel with using acetic acid of 5.94 %mol. The composite was freeze-dried before the pyrolysis and subsequently nitridation.

According to Figure 4.29, XRD patterns show that the sample prepared with silica sol in the content of 2.82 %mol contained only SiC, while the other sample (i.e., silica content of 6.90 %mol) was SiC mixed with Si₃N₄. For the product with silica content of 2.82 %mol, the surface area of the nitrated product after being calcined was much lower than that of the pyrolyzed composite before being nitrated (see Table 4.9). This was expected because the pyrolyzed composite contained a lot of carbon. So, after calcination, the carbon was burnt out leaving only SiC with lower surface area. However, for the sample with the silica content of 6.90 %mol, the surface area of the final product was increased. It was suggested that the pore occurred from the agglomeration of particles with higher silica and carbon content. It should also be noted that the samples in the form of solid piece had lower surface area than that of the powder samples due to the N₂ diffused into the powder samples easier to react with SiO₂ and carbon to form a final products. And the lost reactant (i.e., carbon and SiO (vapor) which was reduced from SiO₂) resulted in high surface area and porosity of the product.

Table 4.9 Surface area and pore properties of the nitrated products after calcination process. The composite was prepared from pre-formed silica sol: 2.82 (a), 6.90 %mol (b), and RF gel aged at 0°C and subjected to various drying before being pyrolyzed and subsequently nitrated. The samples were divided into 2 parts, i.e. crushed powder and solid specimens before subjected in the nitridation process.

Silica content (%mol)	Surface area (m ² /g)		Pore diameter (nm)		Pore volume (cm ³ /g)	
	Powder	Solid specimen	Powder	Solid specimen	Powder	Solid specimen
2.82	32.88	30.97	3.708	3.662	0.031	0.030
6.90	100.66	87.35	2.838	2.877	0.071	0.063

Figure 4.30 and 4.31 presents SEM micrographs of the nitrated products, prepared by using pre-formed silica sol with the silica content of 2.82 and 6.90 %mol, respectively. Both samples were prepared by using freeze drying. At the surface of the product in the form of solid piece, as shown in Figure 4.30(a), large rods of SiC were formed which led to the small surface area. In the middle of the piece (Figure 4.30(b)), it can be observed that there was a rod-like structure. As shown in Figure 4.31, rough grain can be seen in the middle of the sample with silica content of 6.90 %mol.

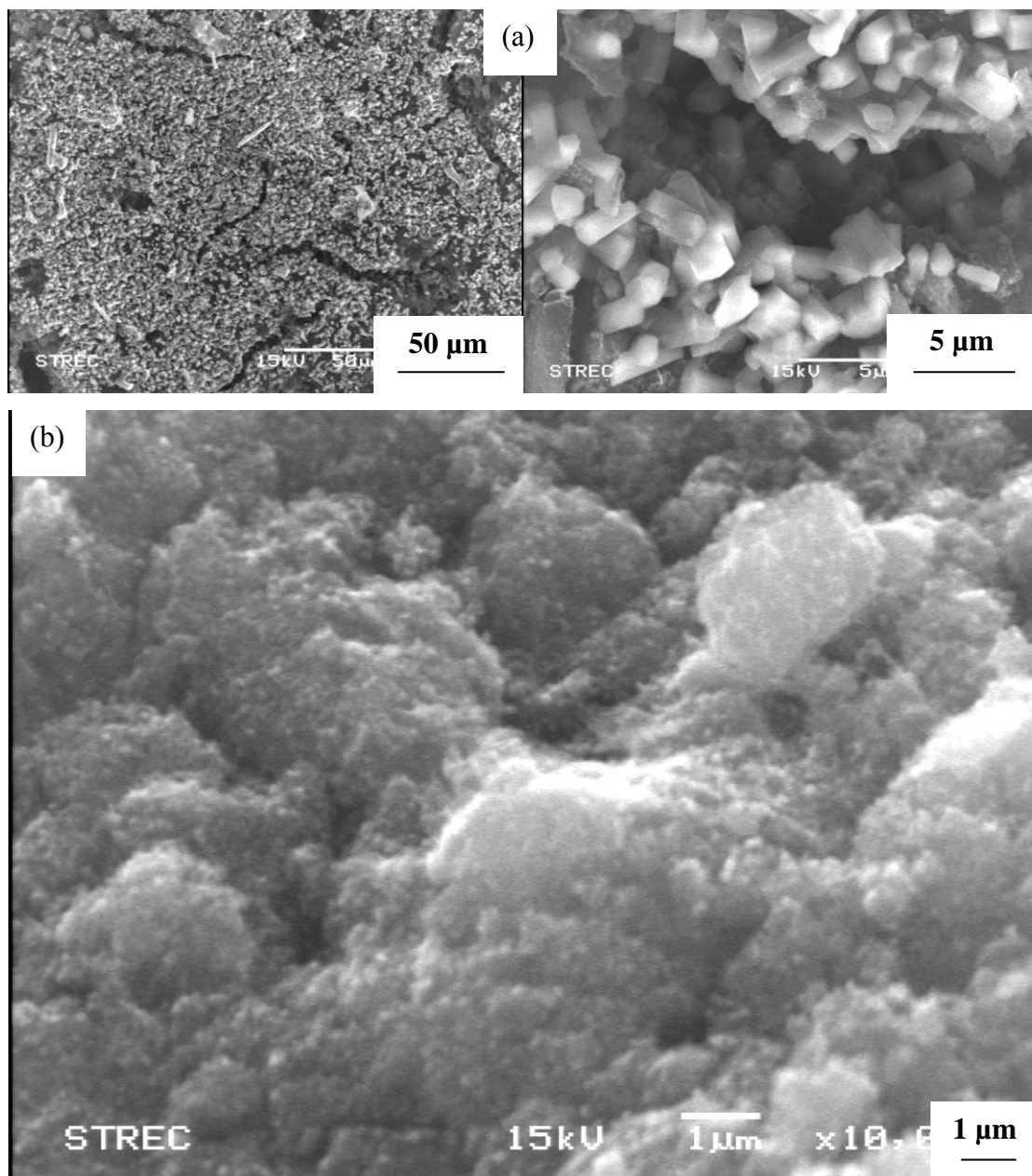


Figure 4.30: SEM micrographs of the nitrated product in the form of solid piece, prepared from pre-formed silica sol with the silica content of 2.82 %mol and RF gel without using acetic acid. The micrographs were taken at the surface (a) and in the center (b) of the specimen.

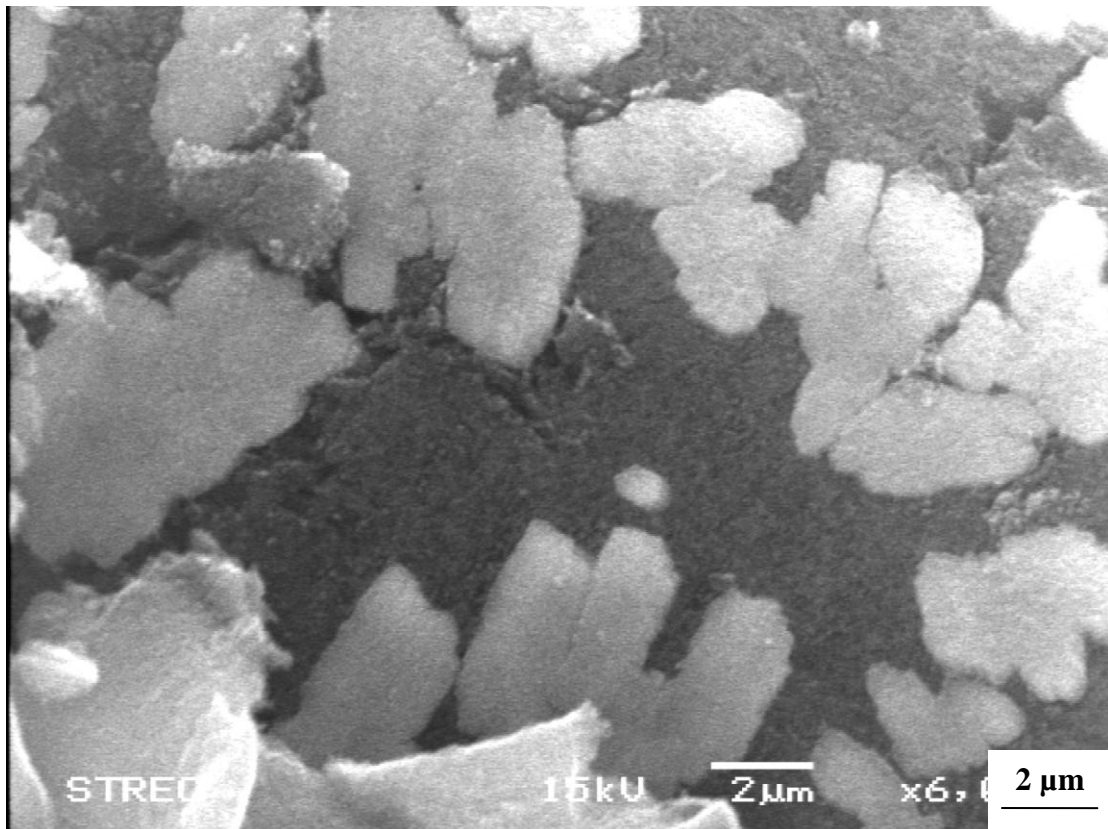


Figure 4.31: SEM micrographs of the nitrided product in the form of solid piece, prepared from pre-formed silica sol with the silica content of 6.90 %mol and RF gel with acetic acid content of 5.94 %mol. The micrographs were taken in the center of the specimen.

CHAPTER V

CONCLUSIONS AND RECOMMENDATIONS

5.1 Summary of the results

1. Porous silicon nitride can be fabricated from silica/RF gel composite via the carbothermal reduction and nitridation. Although most products synthesized in this work are mainly silicon nitride in α -phase, some products produced are mixed with silicon carbide.
2. Strong reaction between APTMS and RF solution is self-propagation, leading to rapid solidification of the gel, which results in low amount of silica precursor that can be introduced to the composite.
3. Acetic acid can be used as an inhibitor for the APTMS/RF gel reaction by breaking the cross-linking network in RF sol. With increasing acetic acid content, more silica can be added to the gel allowed. However, the product obtained becomes denser.
4. Low temperature of RF gel can slow down the reaction so that more silica can be added to the composite. Nevertheless, the surface area of the product is lower than the product which is aged at room temperature.
5. Drying process is one of the parameters which controlling the porosity and particle size of the products. Freeze drying provides higher surface area and total pore volume in the product.
6. The use of pre-formed silica sol is an alternative route to avoid strong reaction between APTMS and RF gel. The result shows that higher silica content can be introduced to the composite, but decreasing in surface area is observed.

5.2 Conclusions

Carbothermal reduction and nitridation is the one of easiest method to fabricate porous silicon nitride but the disadvantage of this method is the less silica precursor content in the composite, due to the violent reaction between carbon source (RF gel) and silica precursor (APTMS). The resulting product is a fragile composite that cannot be formed into solid specimen. So, the investigated effects (i.e., RF aging temperature, acetic acid, the use of pre-formed silica sol as source) allow introduction of higher content of silica precursor into the composite by retarding the reaction between RF gel and APTMS. Drying method controls the surface area and total pore volume to be high and still porous.

5.3 Recommendations for Future Work

Synthesis of porous silicon nitride from silica/RF gel composite via the carbothermal reduction and nitridation process as well as effects of various parameters, such as acetic acid, temperature, type of silica precursor (i.e., APTMS solution and silica sol), and drying process have been investigated. Some recommendations for future work are listed as follows:

1. The optimum acetic acid should be used with silica sol to control surface area and total pore volume and also fabricate into monolith form.
2. Formation of silica/RF gel in shaped articles should be further investigated.

REFERENCES

- [1] Kawai, C., Yamakawa, A. Effect of porosity and microstructure on the strength of Si_3N_4 : designed microstructure for high strength, high thermal shock resistance, and facile machining. Journal of the American Ceramic Society **80** (1997): 2705-2708.
- [2] David W. Richardson., D.W.F. Ceramic Industry. Advancing Advanced Ceramics and Glasses 1-6.
- [3] Jiang, J.-Z., Kragh, F., Frost, D.-J., Lindelov, H. Hardness and thermal stability of cubic silicon nitride. Journal of Physics Condensed Matter **13** (2001): 515-520.
- [4] Matovic, B. Low temperature sintering additive for silicon nitride. Max-Planck-Institut für Metallforschung Stuttgart (2003): 1-133.
- [5] Yang, J.-F., Ohji, T., Zeng, Y.-P., Kanzaki, S., Zhang, G.-J. Fabrication and mechanical properties of porous silicon nitride ceramics from low-purity powder. Ceramics Society of Japan **111** (2003): 758-761.
- [6] Lee, J.-S., Mun, J.-H., Han, B.-D., Kim, H.-D. Effect of $\beta\text{-Si}_3\text{N}_4$ seed particles on the property of sintered reaction-bonded silicon nitride Ceramics International **29** (2003): 897-905.
- [7] Jia, L., Gu, J.-H., Zhang, Y. Preparation of porous Si_3N_4 ceramics with $\beta\text{-Si}_3\text{N}_4$ as seeds. Journal of Synthetic Crystals **37** (2008): 1224-1227.
- [8] Pekala, R.W. Organic aerogels from the polycondensation of resorcinol with formaldehyde. Journal of Materials Science (1989): 3221-3227.
- [9] Soignard, E., et al. High pressure-high temperature investigation of the stability of nitride spinels in the systems $\text{Si}_3\text{N}_4\text{-Ge}_3\text{N}_4$. Solid State Communications **120** (2001): 237-242.
- [10] Melendez-Martinez, J.J. and A. Dominguez-Rodriguez. Creep of silicon nitride. Progress in Materials Science **49** (2004): 19-107.
- [11] Turkdogan, E.T., Bills, P. M., Tippett, V. A. Silicon nitrides: Some physico-chemical properties. Journal of Apply Chemistry **8** (1996): 296-302.
- [12] Riley, F.L. Silicon nitride and related. J. Am. Ceram. Soc **83** (2000): 245-65.
- [13] Xu, M., et al. Theoretical prediction of electronic structures and optical properties of Y-doped $\gamma\text{-Si}_3\text{N}_4$. Physica B: Condensed Matter **403** (2008): 2515-2520.
- [14] Monteverde, F. and A. Bellosi. Effect of the addition of silicon nitride on sintering behaviour and microstructure of zirconium diboride. Scripta Materialia **46** (2002): 223-228.

- [15] Bai, L., et al. Comparative study of β - Si_3N_4 powders prepared by SHS sintered by spark plasma sintering and hot pressing. Journal of University of Science and Technology Beijing, Mineral, Metallurgy, Material **14** (2007): 271-275.
- [16] Ziegler, G. and G. Wotting. Post-treatment of pre-sintered silicon nitride by hot isostatic pressing. International Journal of High Technology Ceramics **1** (1985): 31-58.
- [17] Zeigler, G., Heinrich, J., Wotting, G. Review: Relationships between processing, microstructure and properties of dense and reaction-bonded silicon nitride. Journal of Materials Science **22** (1987): 3041-3086.
- [18] Diaz, A., Redington, W., Kampshire, S. Effect of porosity on properties of Si_3N_4 . Key Engineering Materials **206-213** (2001): 1033-1036.
- [19] Weimer, A.W., Eisman, G. A., Susnitzky, D. W., Beaman, D. R., Mccoy, J. W. Mechanism and kinetics of the carbothermal nitridation synthesis of alpha-Silicon Nitride. Journal of the American Ceramic Society **80** (1997): 2853-2863.
- [20] Yang, J.-F., et al. Synthesis of fibrous β - Si_3N_4 structured porous ceramics using carbothermal nitridation of silica. Acta Materialia **53** (2005): 2981-2990.
- [21] Yang, J., Yang, J.-F., Ohji, T., Shan, S.-Y., Gao, J.-Q. Effect of sintering additives on microstructure and mechanical properties of porous silicon nitride ceramics. Journal of the American Ceramic Society **89** (2006): 3843-3845.
- [22] Karakus, N., A.O. Kurt, and H.o. Toplan. Synthesizing high α -phase Si_3N_4 powders containing sintering additives. Ceramics International **35** (2009): 2381-2385.
- [23] Yang, H., G. Yang, and R. Yuan. Densification and α/β phase transformation of Si_3N_4 containing MgO and CeO_2 during sintering. Materials Chemistry and Physics **55** (1998): 164-166.
- [24] Yamamoto, T., Nishimura, T., Suzuki, T., Tamon, H. Effect of drying method on mesoporosity of resorcinol-formaldehyde drygel and carbon gel. Drying Technology **19** (2001): 1319-1333.
- [25] Tamon, H., Ishizaka, H. Porous characterization of carbon aerogels. Carbon **36** (1998): 1397-1409.
- [26] Shaheen, A., Mihtaseb, Al., Ritter, J. A. Preparation and properties of resorcinol-formaldehyde organic and carbon gels. Advanced Materials **15** (2003): 101-114.
- [27] Yamamoto, T., Mukai, S. R., Endo, A., Nakaiwa, M., Tamon, H. Interpretation of structure formation during the sol-gel transition of a resorcinol-formaldehyde solution by population balance. Journal of Colloid and Interface Science **264** (2003): 532-537.
- [28] Leonard, A., et al. Evolution of mechanical properties and final textural properties of resorcinol-formaldehyde xerogels during ambient air drying. Journal of Non-Crystalline Solids **354** (2008): 831-838.

- [29] Yoshimune, M., et al. Preparation of highly mesoporous carbon membranes via a sol-gel process using resorcinol and formaldehyde. Carbon **46** (2008): 1031-1036.
- [30] Siyasukh, A., et al. Preparation of a carbon monolith with hierarchical porous structure by ultrasonic irradiation followed by carbonization, physical and chemical activation. Carbon **46** (2008): 1309-1315.
- [31] Horikawa, T., J.i. Hayashi, and K. Muroyama. Size control and characterization of spherical carbon aerogel particles from resorcinol-formaldehyde resin. Carbon **42** (2004): 169-175.
- [32] Kraiwattanawong, K., H. Tamon, and P. Praserttham. Influence of solvent species used in solvent exchange for preparation of mesoporous carbon xerogels from resorcinol and formaldehyde via subcritical drying. Microporous and Mesoporous Materials **In Press, Corrected Proof** (2010).
- [33] Schaefer, D.W., Pekala, R., Beaucage, G. Origin of porosity in resorcinol-formaldehyde aerogels. Journal of Non-Crystalline Solids (1995): 159-167.
- [34] Liang, C., G. Sha, and S. Guo. Resorcinol-formaldehyde aerogels prepared by supercritical acetone drying. Journal of Non-Crystalline Solids **271** (2000): 167-170.
- [35] Tamon, H., Ishizaka, H., Yamamoto, T., Suzuki, T. Preparation of mesoporous carbon by freeze drying. Carbon **37** (1999): 2049-2055.
- [36] Czakkel, O., Marthi, K., Geissler, E., Laszlo, K. Influence of drying on the morphology of resorcinol-formaldehyde-based carbon gels. Microporous and Mesoporous Materials **86** (2005): 124-133.
- [37] Job, N., et al. Synthesis optimization of organic xerogels produced from convective air-drying of resorcinol-formaldehyde gels. Journal of Non-Crystalline Solids **352** (2006): 24-34.
- [38] Aguado-Serrano, J., et al. Silica/C composites prepared by the sol-gel method. Influence of the synthesis parameters on textural characteristics. Microporous and Mesoporous Materials **74** (2004): 111-119.
- [39] Xu, H., et al. Porous carbon/silica composite monoliths derived from resorcinol-formaldehyde/TEOS. Journal of Non-Crystalline Solids **356** (2009): 971-976.
- [40] Long, D.-h., et al. Preparation and microstructure control of carbon aerogels produced using m-cresol mediated sol-gel polymerization of phenol and furfural. New Carbon Materials **23** (2008): 165-170.
- [41] Burket, C.L., et al. Genesis of porosity in polyfurfuryl alcohol derived nanoporous carbon. Carbon **44** (2006): 2957-2963.

- [42] Zarbin, A.J.G., R. Bertholdo, and M.A.F.C. Oliveira. Preparation, characterization and pyrolysis of poly(furfuryl alcohol)/porous silica glass nanocomposites: novel route to carbon template. Carbon **40** (2002): 2413-2422.
- [43] Luyjew, K., Tonanon, N., Pavarajarn, V. Mesoporous silicon nitride synthesis via the carbothermal reduction and nitridation of carbonized silica/RF gel composited. Journal of the American Ceramic Society **91** (2008): 1365-1368.
- [44] Zhang, W., H. Wang, and Z. Jin. Gel casting and properties of porous silicon carbide/silicon nitride composite ceramics. Materials Letters **59** (2005): 250-256.
- [45] Thovicha, M. and V. Pavarajarn. Fabrication of mesoporous titanium dioxide assisted by Resorcinol/Formaldehyde gel. Master degree Chemical engineering Chulalongkorn university, 2010.
- [46] Poumuang, C. and V. Pavarajarn. Incorporation of silica into RF gel for the synthesis of porous Si₃N₄/SiC composite via the carbothermal reduction and nitridation. Master degree Chemical engineering Chulalongkorn university, 2008.
- [47] Estella, J., et al. Silica xerogels of tailored porosity as support matrix for optical chemical sensors. Simultaneous effect of pH, ethanol:TEOS and water:TEOS molar ratios, and synthesis temperature on gelation time, and textural and structural properties. Journal of Non-Crystalline Solids **353** (2007): 286-294.
- [48] Jin, G.-Q. and X.-Y. Guo. Synthesis and characterization of mesoporous silicon carbide. Microporous and Mesoporous Materials **60** (2003): 207-212.
- [49] Cheng, T.W. and C.W. Hsu. A study of silicon carbide synthesis from waste serpentine. Chemosphere **64** (2006): 510-514.
- [50] Chen, S.-H. and C.-I. Lin. Phase Transformations in Silicon-containing Solid Sample During Synthesis of Silicon Carbide Through Carbothermal Reduction of Silicon Dioxide. Journal of Materials Science Letters **17** (1998): 657-659.
- [51] Chrysanthou, A., P. Grieveson, and A. Jha. Formation of silicon carbide whiskers and their microstructure. JOURNAL OF MATERIALS SCIENCE **26** (1991): 3463-3476.
- [52] Lin, S.-Y. Hydrogen-induced electronic states and vibrational modes in hydrogenated amorphous silicon nitride. Thin Solid Films **395** (2001): 101-104.
- [53] Ballarini, V., et al. New insights on amorphous silicon-nitride microcavities. Physica E: Low-dimensional Systems and Nanostructures **16** (2003): 591-595.
- [54] Xu, Q., et al. Indoor formaldehyde removal by thermal catalyst: kinetic characteristics, key parameters, and temperature influence. Environ Sci Technol **45** (2011): 5754-5760.
- [55] Karmakar, B., G. De, and D. Ganguli. Dense silica microspheres from organic and inorganic acid hydrolysis of TEOS. Journal of Non-Crystalline Solids **272** (2000): 119-126.

- [56] Yamamoto, F. and R.L. Cunha. Acid gelation of gellan: Effect of final pH and heat treatment conditions. Carbohydrate Polymers **68** (2007): 517-527.
- [57] Lin, C. and J.A. Ritter. Effect of synthesis pH on the structure of carbon xerogels. Carbon **35** (1997): 1271-1278.
- [58] Gonzalez, R.D., T. Lopez, and R. Gomez. Sol-Gel preparation of supported metal catalysts. Catalysis Today **35** (1997): 293-317.
- [59] Al-Oweini, R. and H. El-Rassy. Synthesis and characterization by FTIR spectroscopy of silica aerogels prepared using several Si(OR)₄ and RⁿSi(OR')₃ precursors. Journal of Molecular Structure **919** (2009): 140-145.
- [60] Ida, P., Matjaz, K. Characterization of Phenol-Formaldehyde Prepolymer REsins by In Line FT-IR Spectroscopy. Acta Chim. Slov. **52** (2005): 238-244.
- [61] Yamamoto, T., et al. Effect of drying conditions on mesoporosity of carbon precursors prepared by sol-gel polycondensation and freeze drying. Carbon **39** (2001): 2374-2376.
- [62] Asomoza, M., et al. Hydrolysis catalyst effect on sol-gel silica structure. Materials Letters **36** (1998): 249-253.
- [63] Lopez, T., et al. Spectroscopic characterization of sol-gel silica obtained by electron irradiation. Materials Letters **38** (1999): 1-5.
- [64] López, T., et al. Thermal decomposition and FTIR study of pyridine adsorption on Pt/SiO₂ sonogel catalysts. Thermochimica Acta **255** (1995): 319-328.

APPENDICES

APPENDIX A

CALCULATION OF MOLAR RATIO OF SILICON AND CARBON IN RF GEL COMPOSITE

2.7 g of Resorcinol ($C_6H_4(OH)_2$)

↓ $\div 110$ (M_w of $C_6H_4(OH)_2$)

0.025 mol of $C_6H_4(OH)_2$

↓ 6 mol of C = 1 mol of $C_6H_4(OH)_2$

0.147 mol of C in Resorcinol

0.0106 g of Na_2CO_3

↓ $\div 106$ (M_w of Na_2CO_3)

0.0001 mol of Na_2CO_3

↓ 1 mol of C = 1 mol of Na_2CO_3

0.0001 mol of C in Na_2CO_3

2.8536 g of Formaldehyde (HCHO)

↓ $\div 30.03$ (M_w of HCHO)

0.095 mol of HCHO

↓ 1 mol of C = 1 mol of HCHO

0.095 mol of C in HCHO

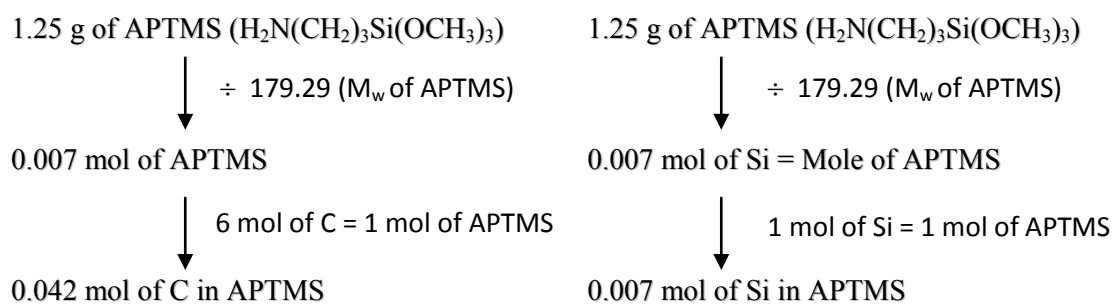
0.2098 g of acetic acid (CH_3COOH)

↓ $\div 60$ (M_w of CH_3COOH)

0.0035 mol of acetic acid

↓ 2 mol of C = 1 mol of CH_3COOH

0.007 mol of C in acetic acid



Molar ratio of silica and carbon =

$$\frac{\text{Mole of Si in APTMS}}{\text{Mole of C in Resorcinol} + \text{Mole of C in HCHO} + \text{Mole of C in Na}_2\text{CO}_3 + \text{Mole of C in CH}_3\text{COOH} + \text{Mole of C in APTMS}}$$

$$\begin{aligned} \text{Molar ratio of silica and carbon} &= \frac{0.007}{0.147 + 0.095 + 0.0001 + 0.007 + 0.042} \\ &= 0.024 \end{aligned}$$

APPENDIX B

DATA OF SURFACE AREA AND AVG. PORE DIAMETER

Table B.1 Data of surface area and average pore diameter of carbonized RF gel aged at 0°C for 6 hour with air convectional drying and freeze drying.

Drying process	Surface area (m ² /g)	Average pore diameter (nm)
Air Drying	368.63	2.0826
Freeze drying	341.52	2.2395

Table B.2 Data of surface area and average pore diameter of carbonized RF gel aged at 25°C with air convectional drying and freeze drying.

Drying process	Surface area (m ² /g)	Average pore diameter (nm)
Air Drying	230.85	1.957
Freeze drying	371.04	2.274

Table B.3 Data of surface area and average pore diameter of pure silica sol with air convectional drying.

Drying process	Surface area (m ² /g)	Average pore diameter (nm)
Air drying	77.523	0.3235

Table B.4 Data of surface area and average pore diameter of silica/RF composite at different temperature with fraction of acetic acid of 10.2 %vol and dried by air convectional drying.

Temperature (°C)	Surface area (m ² /g)	Average pore diameter (nm)
0	2.4545	6.3661
5	1.3790	25.085
10	1.9677	8.2122
25	3.1565	5.8249

Table B.5 Data of surface area and average pore diameter of silica/RF composite at different temperature with fraction of acetic acid of 10.2 %vol and dried by freeze drying.

Temperature (°C)	Surface area (m ² /g)	Average pore diameter (nm)
0	1.4047	8.0116
5	3.0055	10.976
10	1.6221	11.304
25	2.6712	4.5813

APPENDIX C

CALIBRATION CURVES FOR GAS FLOW METER OF SYNTHESIS GAS

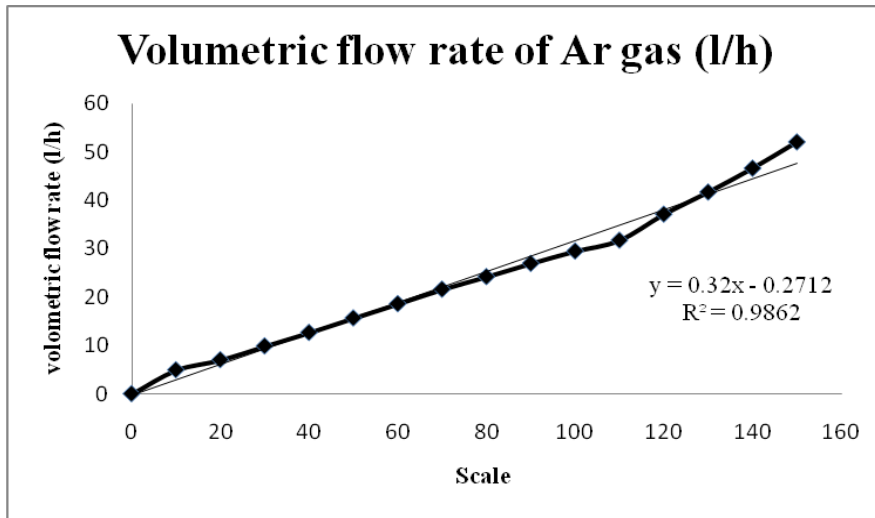


Figure C.1 The calibration curve for argon.

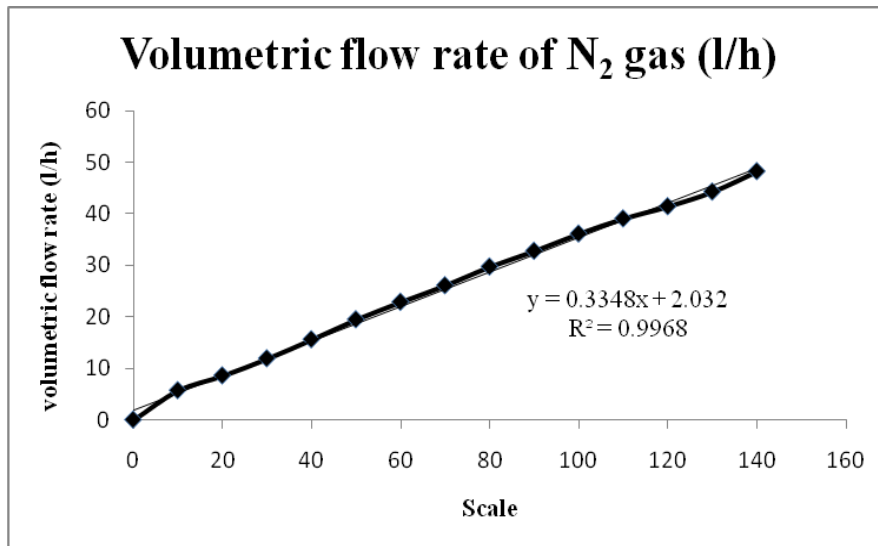


Figure C.2 The calibration curve of nitrogen.

APPENDIX D

SEM MICROGRAPH AND PHOTOGRAPH OF SILICON NITRIDE BEFORE CALCINATION

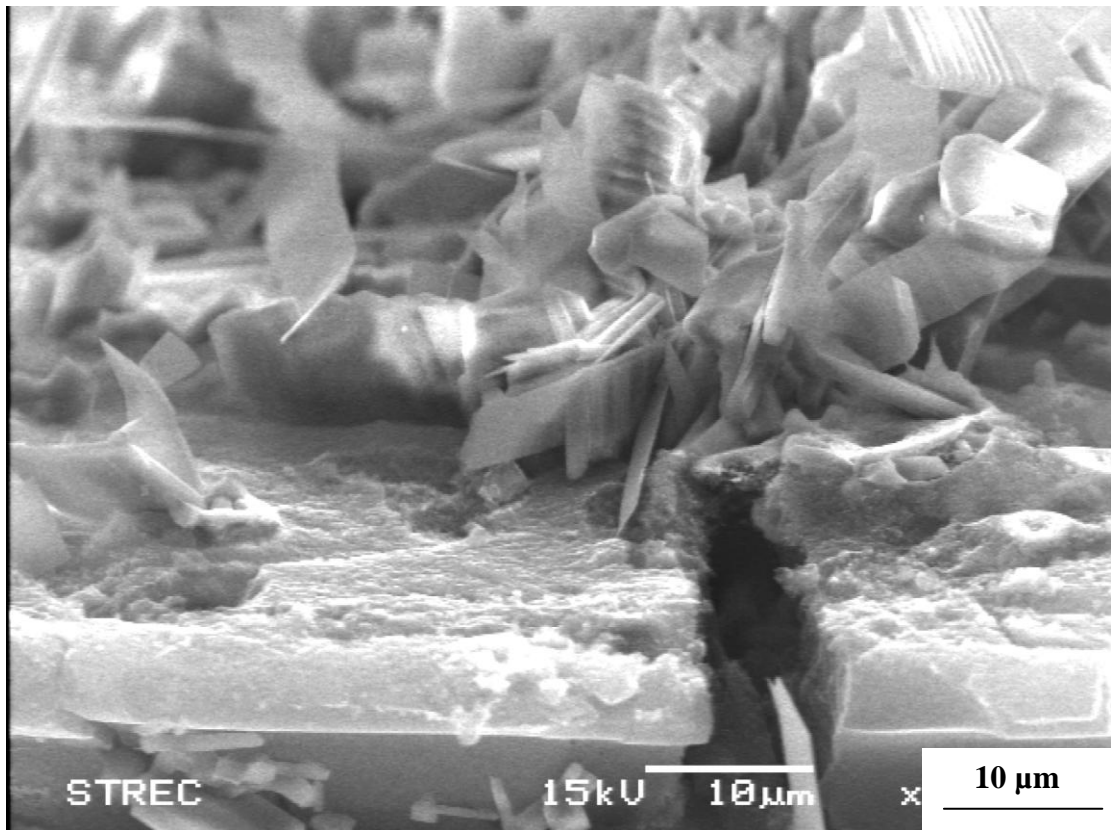


Figure D.1 SEM micrograph of silicon nitride powder by RF/silica composite with fraction of acetic acid of 2.47 %mol dried by freeze drying.



Figure D.2 Photograph of silicon nitride powder synthesized by RF/silica composite with fraction of acetic acid of 2.47 %mol dried by freeze drying.

VITA

Miss. Wischanee Juwarahawong was born on 18 December, 1986, in Bangkok, Thailand. She received the Bachelor's Degree of Engineering with a major in Chemical Engineering from Thammasat University, *Pathumthani* in March 2009. She entered the Master of Engineering in Chemical Engineering at Chulalongkorn University, Bangkok, Thailand in May 2009.

List of publication

1. Wischanee Juwarahawong, Varong Pavarajarn, "Fabrication of Porous Silica/Carbon Composite using RF Gel for Synthesis of Silicon Nitride Specimen via Carbothermal Reduction and Nitridation", the 17th Regional Symposium on Chemical Engineering, Bangkok, Thailand, November 22-23, 2010.